Available online at www.sciencedirect.com
SCIENCE DIRECT®
Computers and Chemical Engineering 27 (2003) 1813–1839
Computers & Chemical Engineering
www.elsevier.com/locate/compchemeng

A strategy for the integration of production planning and reactive scheduling in the optimization of a hydrogen supply network

Susara A. van den Heever, Ignacio E. Grossmann *

Department of Chemical Engineering, Carnegie Mellon University, Pittsburgh, PA 15213, USA

Received 20 September 2002; received in revised form 27 May 2003; accepted 12 June 2003

Abstract

In this paper, we address the integration of production planning and reactive scheduling for the optimization of a hydrogen supply network consisting of five plants, four inter-connected pipelines and 20 customers. We present multiperiod mixed integer nonlinear programming (MINLP) models for both the planning and scheduling levels. The planning model includes complex pricing functions resulting from deregulation, with a simplified pipeline description and determines feed and energy prices, as well as production levels, for a monthly horizon divided into 12-h time periods. Prices are fixed on the scheduling level, while a detailed pipeline model is included, to determine the on/off status and load steps of compressors on an hourly basis, in order to satisfy the actual demands as they become known while adhering to pressure constraints. In addition, we propose a solution methodology where the demand forecast is updated and the planning model is rerun every 12 h, while the scheduling model is run every hour and information is passed between the two levels to facilitate integration. We show that the planning model quickly becomes intractable and propose a heuristic solution method for this level based on Lagrangean decomposition. Results show that the proposed Lagrangean decomposition heuristic reduces the computational effort for solving the planning model by more than an order of magnitude compared to the commercial MINLP solver DICOPT++. It is also shown that for the majority of the plants, the power consumption and hydrogen production from the scheduling level agrees with the planning level. In some cases, however, the integration is hampered by the presence of nonlinearities, especially on the scheduling level, that lead to suboptimal or infeasible solutions. These nonlinearities need to be further addressed before the proposed methodology can be implemented in practice.

Keywords: Planning; Scheduling; Pipeline; Optimization

1. Introduction

The integration of planning and scheduling in optimization has received increasing attention in recent years (e.g. Birewar & Grossmann, 1990; Coxhead, 1994; Papageorgiou & Pantelides, 1996a; Papageorgiou and Pantelides, 1996b; Petkov & Maranas, 1997; Sand, Engell, Märkert, Schultz & Schulz, 2000; Rodrigues, Latre & Rodrigues, 2000; Lasschuit and Thijssen, 2003; Neiro and Pinto, 2003). This trend follows the realization in industry that planning and scheduling decisions need to be considered simultaneously to gain a competitive advantage (see e.g. Shobrys and White, 2000). Two of the major challenges towards this integration are dealing with the different time scales and with the problem size of the resulting optimization model. In this work, we address these challenges by considering the integration of production planning and reactive scheduling in the optimization of a hydrogen supply network. An additional challenge that arises is the modeling and solution of the pipeline system. Pipeline flow models are difficult to solve due to the presence of nonlinear functions such as absolute values, signs (+ or −), and flow transitions that result in discontinuities and other non-convexities. It is, however, important to include these details in the model to ensure feasible flows and to satisfy customer demands and minimum contract pressure levels.

* Corresponding author. Tel.: +1-412-268-2230; fax: +1-412-268-7139.

E-mail addresses: susara@andrew.cmu.edu (S.A. van den Heever), grossmann@cmu.edu (I.E. Grossmann).

0098-1354/03/$ - see front matter
doi:10.1016/S0098-1354(03)00158-3

Nomenclature

Sets:

J	plants
OG(J)	offgas plants
OD(J)	on-demand plants
K	compressors
iden_$k(K,K')$	compressors K and K' are identical
A	compressor load steps
L	pipelines
H2$L(L)$	hydrogen pipelines
OG$L(L)$	offgas pipelines
TG$L(L)$	tailgas pipelines
k_config(K,J,L)	configuration of compressor K associated with plant J and pipeline L
c^2 (K,J,L)	compressors with control structure 2
C	customers
T	time periods
T^{on} (T)	on-peak time periods
T^{off} (T)	off-peak time periods
N^{peak}	number of peaks to be used in energy price calculation
N	pipeline nodes
N_pipe$(H2L,N)$	node N associated with pipeline $H2L$
P_node(J,N)	plant P flowing into node N
C_node(C,N)	customer C flowing out of node N
arc(n,n')	arc between node n and n'
PCV(N,N')	arc N to N' is a pressure control valve

Indices:

j	plants $j \in J$
k	compressor $k \in K$
a	load step $a \in A$
l	pipeline $l \in L$
c	customer $c \in C$
t	time period $t \in T$
n^{peak}	peak period $n^{\mathrm{peak}} \in N^{\mathrm{peak}}$
n	node $n \in N$

Parameters:

$a^{\mathrm{turb}}_{n,n'}$	coefficient for calculating turbulent Reynolds number
a_{0j}, a_{1j}, a_{2j}, a_{3j}	coefficients for calculating natural gas flow for on demand plant j
a^{NGM}_j	first coefficient for calculating NGM_j
annon_j	on peak average power usage for the past 12 months for plant j
aux^1_j, aux^2_j, aux^3_j	coefficients for calculating auxiliary power used by plant j
$b^{\mathrm{turb}}_{n,n'}$	coefficient for calculating turbulent Reynolds number
b_{0j}, b_{1j}, b_{2j}	coefficients for calculating steam flow for on demand plant j
b^{NGM}_j	second coefficient for calculating NGM_j
$c^{\mathrm{turb}}_{n,n'}$	coefficient for calculating turbulent Reynolds number
c^{dPdz}	conversion factor for driving force calculation
$c^{\mathrm{powercost}}$	factor for power cost calculation
c^{base}_j	base cost coefficient for power cost calculation for plant j
c^{NGPrice}_j	constant including natural gas price for offgas plant j
c^{prim}_j	primary cost coefficient for power cost calculation for plant j
c^{recov}_j	constant used for H_2 recovery calculation for offgas plant j
c^{scnd}_j	secondary cost coefficient for power cost calculation for plant j
c^{steam}_j	correction factor for steam calculation for on demand plant j
$\mathrm{custdem}_{c,l,t}$	demand from customer c on pipeline l in period t

$D_{n,n'}$	diameter of pipe arc between node n and n'
days	days in the planning horizon
duration_t	duration of period t
ECI_j	index for calculating steam credit for on demand plant j
$\text{ECI}_j^{\text{ref}}$	reference index for calculating steam credit for on demand plant j
k^{isen}	isentropic exponent for hydrogen at average conditions
FERC_j	index for calculating natural gas price for plant j
$\text{flow}_{akjl}^{\text{load}}$	flow rate at reference conditions in load step a at compressor k at plant j to pipeline l
$\text{H}_2\text{flow}_{jt}^{\text{plan}}$	fixed hydrogen production rate for plant j in period t from the planning level
H_2inter_j	intermediate value for H_2 flow for offgas plant j
$\text{H}_{2j}^{\max}$	maximum hourly H_2 flow from plant j
$\text{H}_{2j}^{\min}$	minimum hourly H_2 flow from plant j
$\text{H}_{2j}^{\text{og,comp}}$	H_2 composition in feed to offgas plant j
H_2ogpro_j	total H_2 flow to the offgas provider from plant j over planning horizon
$\text{H}_2\text{purity}_j$	H_2 purity for offgas plant j
inv_n^0	initial inventory associated with node n
$L_{n,n'}$	length of pipe arc between nodes n and n'
L_{kjl}^{flow}	lower bound on flow rate through compressor k at plant j to pipeline l
L_j^{H2flow}	lower bound on H_2 flow rate produced by plant j
M	molecular weight of H_2
$\text{min}_j^{\text{pKVA}}$	minimum value for primKVA in energy price calculation for plant j
ngflow1_j	parameter for calculating natural gas price for on demand plant j
ngflow2_j	parameter for calculating natural gas price for on demand plant j
ngflow3_j	parameter for calculating natural gas price for on demand plant j
OGM_j	offgas multiplier for calculating offgas price for plant j
$P_{kjlt}^{\text{dis,max}}$	maximum discharge pressure for compressor k at plant j to pipeline l in period t
$P_{kjt}^{\text{dis,ref}}$	Discharge pressure for compressor k at plant j to pipeline l at reference conditions
P_{kjl}^{feed}	feed pressure into compressor k at plant j to pipeline l
$P_{kjl}^{\text{suc,ref}}$	suction pressure for compressor k at plant j to pipeline l in period t at reference conditions
peakfrac_j	fraction used in energy price calculation
$\text{plantpower}_{jt}^{\text{plan}}$	plantpower target from planning level for scheduling level
$\text{power}_{akjl}^{\text{load}}$	power at reference conditions in load step a for compressor k at plant j to pipeline l
R_{g}	gas coefficient
T_{abs}	absolute temperature
T_{kjl}^{suc}	suction temperature for compressor k at plant j to pipeline l in period t
$T_{kjl}^{\text{suc,ref}}$	suction temperature for compressor k at plant j to pipeline l in period t at reference conditions
U_{kjl}^{flow}	upper bound on flow through compressor k at plant j to pipeline l
$U_{kjl}^{\text{flow,r}}$	upper bound on recycle flow through compressor k at plant j to pipeline l
U_j^{H2flow}	upper bound on H_2 flow produced by plant j
$U_j^{\text{st,exp}}$	upper bound on the amount of steam exported from on demand plant j
α_j^{steam}	parameter for calculating steam credit for on demand plant j
ΔFERC1_j	parameter for calculating natural gas price for on demand plant j
ΔFERC2_j	parameter for calculating natural gas price for on demand plant j
ΔFERC3_j	parameter for calculating natural gas price for on demand plant j
ΔFERC4_j	parameter for calculating natural gas price for on demand plant j
$\varepsilon_{n,n'}$	roughness of arc between n and n'
η_{kjlt}	volumetric efficiency of compressor k at plant j to pipeline l
η_{kjl}^{ref}	volumetric efficiency of compressor k at plant j to pipeline l at reference conditions
μ	viscosity of H_2
Variables:	
Continuous variables:	
$\text{Absflow}_{n,n',t}$	absolute value of flow rate in arc n to n' in period t

$\mathrm{Auxpower}_{jt}$	auxiliary power used by plant j in period t
$\mathrm{Avgpower}_{j}$	average periodic power consumption for plant j
$\mathrm{Custflow}_{nt}$	H_2 flow rate from node n to a customer in period t
$\mathrm{dPdz}_{n,n',t}$	driving force for flow in arc from n to n' in period t
$f_{n,n',t}$	friction factor for flow in arc from n to n' in period t
$\mathrm{feedcost}_{j}$	feed cost for plant j over planning horizon
flow_{kjlt}	flow rate through compressor k at plant j to pipeline l in period t
$\mathrm{flowarc}_{n,n',t}$	flow rate in arc from n to n' in period t
$\mathrm{flow}_{kjlt}^{\mathrm{comp}}$	flow rate exiting compressor k at plant j to pipeline l in period t
$\mathrm{flow}_{kjlt}^{\mathrm{recy}}$	recycle flow rate for compressor k at plant j to pipeline l in period t
$\mathrm{flow}_{kjlt}^{\mathrm{ref}}$	flow rate at reference conditions through compressor k at plant j to pipeline l in period t
$\mathrm{H_2flow}_{jt}$	total hydrogen flow rate produced by plant j in period t
$\mathrm{H_2flow}_{j}^{\mathrm{tot}}$	total H_2 flow for plant j during planning horizon
$\mathrm{H_2recov}_{jt}$	H_2 recovery in offgas plant j in period t
$\mathrm{Inv}_{n,t}$	inventory associated with node n in period t
$\mathrm{max}_{n\mathrm{peak},j}^{\mathrm{off}}$	n^{peak} largest power peak for off peak production at plant j
$\mathrm{max}_{n\mathrm{peak},j}^{\mathrm{on}}$	n^{peak} largest power peak for on peak production at plant j
$\mathrm{mo}_{j}^{\mathrm{off}}$	average monthly off peak power production for plant j for N^{peak} periods
$\mathrm{mo}_{j}^{\mathrm{on}}$	average monthly on peak power production for plant j for N^{peak} periods
ngflow_{jt}	natural gas flow to on demand plant j in period t
$\mathrm{ngflow}_{j}^{\mathrm{tot}}$	total natural gas flow to on demand plant j during planning horizon
$\mathrm{ngprice}_{j}$	natural gas price for on demand plant j
NGM_{j}	multiplier for calculating offgas price for plant j
$\mathrm{ogflow}_{j,t}$	offgas flow rate for plant j in period t
$\mathrm{ogprice}_{j}$	offgas price for plant j
P_{kjlt}^{dis}	discharge pressure for compressor k at plant j to pipeline l in period t
$P_{n,t}^{\mathrm{node}}$	pressure at node n in period t
$P_{n,n',t}^{\mathrm{arc}}$	pressure in arc from n to n' in t
$P_{h2l,t}^{\mathrm{avg}}$	average pressure in pipeline $h2l$ in period t
P_{kjlt}^{suc}	suction pressure for compressor k at plant j to pipeline l in period t
$\mathrm{pipeflow}_{jlt}$	H_2 flow rate from plant j into pipeline l in period t
$\mathrm{plantflow}_{n,t}$	H_2 flow rate from a plant into node n in period t
$\mathrm{plantpower}_{jt}$	total power required by plant j in period t
power_{kjlt}	power used by compressor k at plant j to pipeline l in period t
$\mathrm{powercost}_{j}$	power cost for plant j during planning horizon
$\mathrm{power}_{kjlt}^{\mathrm{ref}}$	power at reference conditions for compressor k at plant j to pipeline l in period t
$\mathrm{primKVA}_{j}$	primary value in power cost calculation for plant j
$\mathrm{primKWHR}_{j}$	primary value in power cost calculation for plant j
$\mathrm{Re}_{n,n',t}$	Reynolds number in arc from n to n' in period t
$s1_{n,t}^{\mathrm{inv}}$	slack variable for inventory calculation
$s2_{n,t}^{\mathrm{inv}}$	slack variable for inventory calculation
$s1_{jt}^{\mathrm{linkflow}}$	slack variable for flow link between planning and scheduling
$s2_{jt}^{\mathrm{linkflow}}$	slack variable for flow link between planning and scheduling
$s1_{jt}^{\mathrm{linkpower}}$	slack variable for power link between planning and scheduling
$s2_{jt}^{\mathrm{linkpower}}$	slack variable for power link between planning and scheduling
$\mathrm{scndKWHR}_{j}$	secondary value in power cost calculation for plant j
$\mathrm{steamcred}_{j}$	steam credit for on demand plant j for the planning horizon
$\mathrm{steamexp}_{jt}$	steam exported from plant j in period t
$\mathrm{steamflow}_{jt}$	steam flow rate for on demand plant j in period t
$\mathrm{steamrev}_{jt}$	revenue from exported steam from on demand plant j in period t
$\mathrm{steamvent}_{jt}$	steam vented from plant j in period t
tgflow_{jt}	tailgas flow for plant j in period t
$\Delta P_{kjlt}^{\mathrm{suc}}$	pressure change between feed and suction for compressor k at plant j to pipeline l in period t
$\Delta P_{n,n',t}^{\mathrm{valve}}$	pressure drop in pressure control valve from node n to n' in period t

$\rho_{n,t}^{\text{node}}$	density at node n in period t
$\rho_{n,n',t}^{\text{avg}}$	average density between nodes n and n' in period t
Discrete variables:	
y_j^{on}	plant j operates during the planning horizon
y_{jt}	plant j produces hydrogen in period t
z_{akjlt}	compressor k at plant j to pipeline t operates in load step a in period t
$b_j^{1,\text{NGM}}$	binary to calculate NGM_j for offgas plants
$b_j^{2,\text{NGM}}$	binary to calculate NGM_j for offgas plants
$B_j^{1,\text{NGPrice}}$	binary to calculate natural gas price for on demand plants
$b_j^{2,\text{NGPrice}}$	binary to calculate natural gas price for on demand plants
$b_j^{3,\text{NGPrice}}$	binary to calculate natural gas price for on demand plants
$b_j^{4,\text{NGPrice}}$	binary to calculate natural gas price for on demand plants
$b_{j,n\text{peak},t\_\text{on}}^{1,\text{onpeak}}$	binary to determine the N^{peak} largest on-peak power consumptions
$b_{j,n\text{peak},t\_\text{on}}^{2,\text{onpeak}}$	binary to determine the N^{peak} largest on-peak power consumptions
$b_j^{1,\text{pKVA}}$	binary to calculate primKVA for plant j
$b_j^{2,\text{pKVA}}$	binary to calculate primKVA for plant j
$b_j^{3,\text{pKVA}}$	binary to calculate primKVA for plant j

While numerous articles have been published on either planning or scheduling (for a short review see Shah, 1998, and Grossmann, Van den Heever & Harjunkoski, 2001), only a few have addressed the integrated problem. Shobrys and White (2000) emphasize the importance of integrated planning, scheduling and control in industry, and address some non-technical challenges towards this integration, such as human and organizational behavior. On a technical level, Grossmann et al. (2001) discuss the role of optimization methods in achieving integration. These authors emphasize the importance of time representation, present a general disjunctive formulation for integrating planning and scheduling, as well as some techniques for dealing with the large size of integrated models.

Regarding the time representation, one approach is to define a very large scheduling problem that spans the whole planning horizon and defining longer lengths for future time periods to yield a formulation where the immediate future includes more detail than the distant future. Bassett, Dave, Doyle, Kudva, Pekny, Reklaitis, Subramanyam, Miller and Zentner (1996) present such a model and show that it cannot be solved in the full space due to its size and that some type of decomposition is required. To this end, they propose a decomposition scheme where an aggregate planning level is solved, and separate detailed scheduling problems are subsequently solved for each planning period. Their decomposition algorithm ties in with a second approach to time representation for integration, namely to define an aggregate planning problem from which information is passed to a detailed scheduling model. Birewar and Grossmann (1990) propose such models for the simultaneous planning and scheduling of multipurpose batch plants. In their approach, planned production levels can be met within the available cycle time using an aggregate scheduling model. A third method for dealing with the different time scales is to use a rolling horizon approach where only a subset of the planning periods include the detailed scheduling decisions with shorter time increments. The detailed planning/scheduling period moves as the model is solved in time, thus the term ‘rolling horizon’. When such a planning/scheduling model is solved in real-time, the first planning period is often a detailed scheduling model while the future planning periods include only planning decisions and this is also the approach we use in this work. Dimitriadis, Shah and Pantelides (1997) presented RTN-based rolling horizon algorithms for medium term scheduling of multipurpose plants. Sand et al. (2000) use a rolling horizon approach, in combination with a Lagrangean relaxation algorithm, for the solution of a two-level hierarchical planning and scheduling problem where uncertainty has been included explicitly on the planning level.

Other research on the integration of planning and scheduling includes that of Papageorgiou and Pantelides (1996a,b), who propose a bilevel decomposition approach for campaign planning and scheduling of multipurpose batch/semicontinuous plants with scheduling decisions aggregated on the planning level and some planning decisions fixed on the scheduling level. More work on the integration of planning and scheduling for batch plants was carried out by Rodrigues et al. (2000) who propose a multilevel decomposition approach where capacities are determined on the planning level and the scheduling level is based on the STN formulation. Das, Rickard, Shah and Macchietto (2000) discuss this integration by using the same basic data and variables in all models, while information is passed from the higher hierarchical to the lower levels as the models are solved in sequence. Bose and Pekny (2000) proposed a model predictive framework for the planning and scheduling of a consumer goods supply chain. They present an architecture where modules for demand forecasting, optimization, and simulation are integrated to deal with uncertainty in promotional demands. Petkov and Maranas (1997) address uncertainty in demand for batch plants by extending the model of Birewar and Grossmann.

Reactive scheduling can be defined as the problem of updating a schedule dynamically as the constraints or assumptions on which it is based change. The problem at hand is therefore one of reactive scheduling, seeing that the scheduling decisions are adjusted as soon as updated pipeline measurements become available, and not only with each planning period. The reactive scheduling problem we consider in this work is different from the batch processing problems, in the sense that the plants and hydrogen pipeline do not operate in batches. Instead, there is a continuous supply of hydrogen and scheduling decisions involve basic on/off decisions to satisfy the demand as they become known. Coxhead (1994) gives a qualitative description of a similar concept for refinery planning and scheduling. In addition, the reactive scheduling considered here incorporates a complex model for the hydrogen pipeline network, to accurately determine a schedule that satisfies both pressure and flow constraints.

The modeling of gas pipeline networks has been considered by a number of researchers in the past. Most of the work has been carried out for natural gas pipelines. Wong and Larson (1968) proposed a dynamic programming approach for the optimization of a natural gas pipeline system, but consider only a single compressor and single pipeline section and the input flow and internal pressures are fixed. Sood, Punk and Delmastro (1971) consider a similar problem and minimize the energy usage for operation of the compressors as it relates to flow and pressure. A single-period convex MINLP model for gas transmission pipeline synthesis was presented by Duran and Grossmann (1986) and solved for a superstructure of two wells leading to two demand points. This model includes discharge pressures, pipe dimensions, compressor location, and compressor power as variables. Martinez-Benet and Puigjaner (1988) consider the design of large-scale pipeline networks at steady state. While very large pipeline systems are solved in detail with their approach, the purpose of their work is design at steady state and they do not consider the operation of existing systems. Marques and Morari (1988) consider the on-line optimization of a natural gas transmission pipeline network, and contribute to work up to that time by using the compressor discharge pressure as manipulated variable and including the compressor constraints in their model. They link a dynamic pipeline simulator with an optimizing predictive control scheme over a moving horizon. Bullard and Biegler (1992) address discontinuous functions that arise in pipeline network models and present both continuous and mixed-integer versions of a smooth approximation for the max function associated with one-directional flow enforced by checkvalves. Their results show that the mixed-integer formulation requires significantly larger CPU times than the continuous formulation. Türkay and Grossmann (1998) present an example that follows the work by Bullard and Biegler (1992) and propose a disjunctive formulation to model the check valves. This formulation also requires discrete variables and has the potential of getting computationally taxing for large models, although it provides much tighter relaxations. These two sets of authors do not consider the compressor operation. Sun, Uraikul, Chan and Tontiwachwuthikul (1999) consider the optimization of natural gas pipeline operations, including the on/off status of compressors to satisfy demand while minimizing cost. They present an integrated expert system and operations research approach where the expert system is used to determine whether the volume of gas in the pipeline is sufficient to satisfy demands, and a fuzzy 0–1 linear program is used to determine which compressors to switch on or off. They consider a horizon of only 8 h and do not model the pipeline explicitly, but instead use one equation to approximate the volume of gas in the pipeline at an average pressure.

None of the articles on pipeline optimization mentioned in this section consider long enough time horizons to handle the complex pricing of energy and feed implied by deregulation. Neither do they incorporate the possibility of using the pipeline as a storage device that requires good knowledge of the pipeline inventory and thus a detailed pipeline model. In most of these articles, the direction of flow is pre-specified, while flow in a supply network can be in either a positive or a negative direction.

We address these issues by proposing two integrated multiperiod MINLP models for planning and reactive scheduling of the supply system. In addition, we propose a strategy for the integrated solution of these models and a Lagrangean decomposition-based heuristic to deal with the problem size at the planning level. Uncertainty in the demand forecast is partly dealt with in that the reactive scheduling allows changes in operation when demands are different from their predicted values and the planning model and monthly forecast are updated every 12 h as more information becomes known. To the best of our knowledge, the work presented in this paper is unique in combining daily or monthly planning decisions that are essential for the cost minimization of gas pipeline network operations, with hourly reactive scheduling of compressor operation, in an optimization framework. Isothermal conditions are assumed in this work and start-up and shut-down costs are not con-

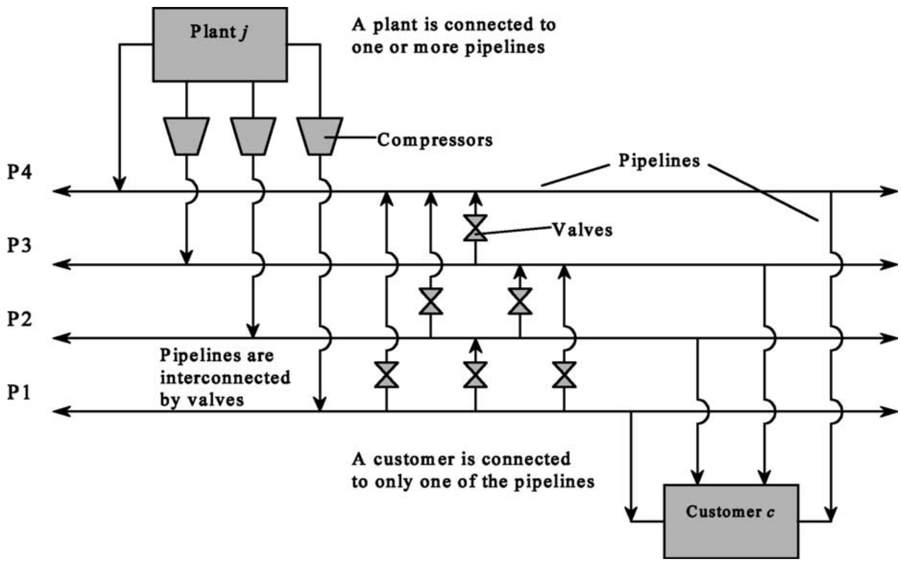

Fig. 1. Network of plants, pipelines and customers.

sidered although these costs can in principle be included without much difficulty.

In Section 2, we present the problem statement. This is followed by the proposed integrated solution methodology and the two optimization models for the planning and scheduling levels, respectively. Example 1 presents a small instance to demonstrate the proposed approach, and a larger instance that demonstrates the need for a specialized solution algorithm on the planning level. This is followed by a section on the proposed Lagrangean decomposition heuristic for the upper level planning model. Example 1 is revisited to demonstrate the performance of the proposed heuristic, while Example 2 demonstrates the performance of the proposed approach, including the planning heuristic, on the largest instance of the supply network. Our findings are summarized in the Section 9.

2. Problem statement

In this work, we address the problem of integrating production planning and reactive scheduling for the optimization of a hydrogen supply network. The network consists of five hydrogen producing plants that feed into a pipeline system at four different pressure levels, $P_1 > P_2 > P_3 > P_4$, that supplies hydrogen to about 20 customers (see Fig. 1) with time varying demands. Although we cannot show the actual customer and pipeline layout due to confidentiality, Fig. 1 shows all possible connections. Each plant can supply hydrogen to multiple pressure levels, but each customer receives hydrogen at only one pressure level. In addition, letdown valves exist that allow the flow of hydrogen from a higher to a lower pressure pipeline.

Of the five plants, three produce hydrogen from refinery offgas, while the other two produce hydrogen from natural gas. Each plant produces hydrogen at one or more of four pressure levels and accordingly has a number of reciprocating compressors, each having multiple load steps.

Production levels need to be determined at each plant for a 1 month planning horizon, with the objective of minimizing costs while satisfying the expected demands. The planning horizon is divided into T 12-h periods, which are characterized as alternating between on- and offpeak. Energy costs for each plant are determined by the N^{peak} highest on- and offpeak power usages, while feed costs for each plant are determined by the total monthly production, leading to complex economic trade-offs. The fact that hydrogen is compressible can be exploited by using the pipeline for inventory purposes. Thus, gas can be produced in a period when production is cheaper, stored in the pipeline and distributed to the customers at a later period. Reactive scheduling of the compressor operation is carried out on an hourly basis to satisfy the actual demand as they become known, subject to the pipeline pressure constraints.

The planning decisions we address are:

a) whether or not each plant operates in each planning period
b) the percentage of time each compressor load step operates in each planning period
c) the hydrogen production levels for each plant in each planning period

d) the power consumption in each planning period

The reactive scheduling decisions are:

a) the exact operating loadstep for each compressor in each scheduling period
b) the discharge pressure and flow for each compressor in each scheduling period
c) production levels and power consumption for each plant in each scheduling period

Our goal is to integrate these two levels of decision making in order to satisfy the planned production and power consumption levels that determine prices, while supplying a feasible operating schedule that satisfies demands.

3. Solution approach

A simultaneous optimization model that involves hourly scheduling decisions and 12-h planning decisions over a month long planning horizon can potentially involve 744 time periods. Given the detailed plant and pipeline descriptions as well as the number of discrete decisions, solving such a model in the full space is not feasible. Some form of decomposition and/or model reduction is therefore required. One option is to define scheduling decisions only for the immediate future, for example for the first 12 h. This would reduce the number of time periods to 73. However, we found that even under such circumstances, the number of discrete decisions lead to an intractable solution, while the chance of obtaining an infeasible solution is increased due to the large number of nonlinear pipeline constraints.

We therefore propose a two-level solution methodology that involves an upper level planning model and a lower level reactive scheduling model. This decomposition is motivated by the realization that the detailed pipeline description, involving items such as pressure gradients and flow transitions, is not required at the planning level where time periods are 12 h long and pipeline pressures can essentially be assumed to be constant during each period. In addition, the detailed price calculations are not required at the scheduling level. A high-level representation of our proposed methodology is shown in Fig. 2 (please refer also to Fig. 13 for a detailed diagram on the Lagrangean decomposition heuristic used on the planning level).

An initial inventory and a demand forecast are the inputs to the planning level. At this level a multiperiod MINLP is solved to determine the hydrogen production and power consumption levels for each time period in order to minimize feed and energy costs. Since the planning periods each have a length of 12 h, the dynamic pipeline constraints are simplified by assuming a constant average pressure at each pressure level. Note that the planning problem is solved one planning period before the actual scheduling is required in order to allow enough time for the solution of the multiperiod MINLP.

From the solution of the planning model, targets for hydrogen production and power consumption for each plant are set for the scheduling model. In addition, the initial state of the first scheduling period is determined from the planning output, although this initial inventory would ideally be estimated online from sensors in the pipeline. Also, the prices for energy and feed are fixed at the scheduling level based on the values from the planning model.

On the scheduling level, ideally a multiperiod MINLP is solved in a rolling horizon strategy to determine the

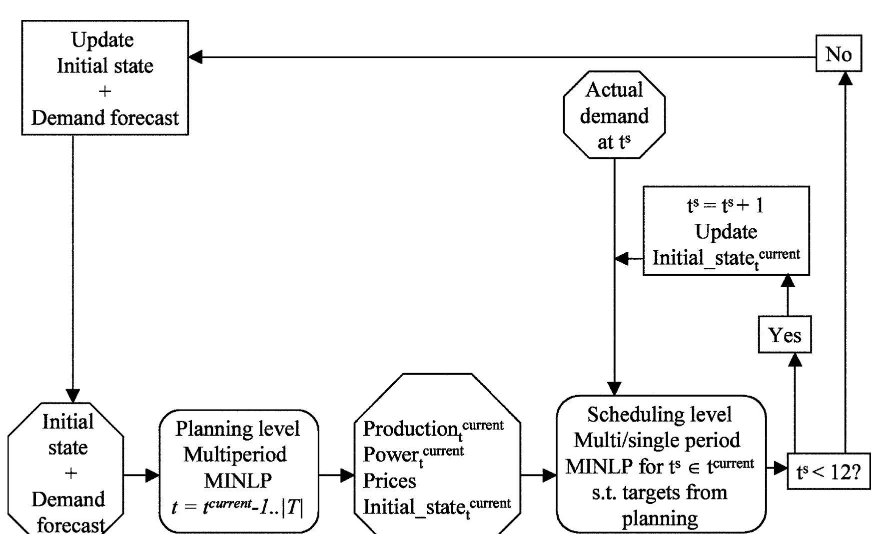

Fig. 2. Solution strategy for two-level decomposition.

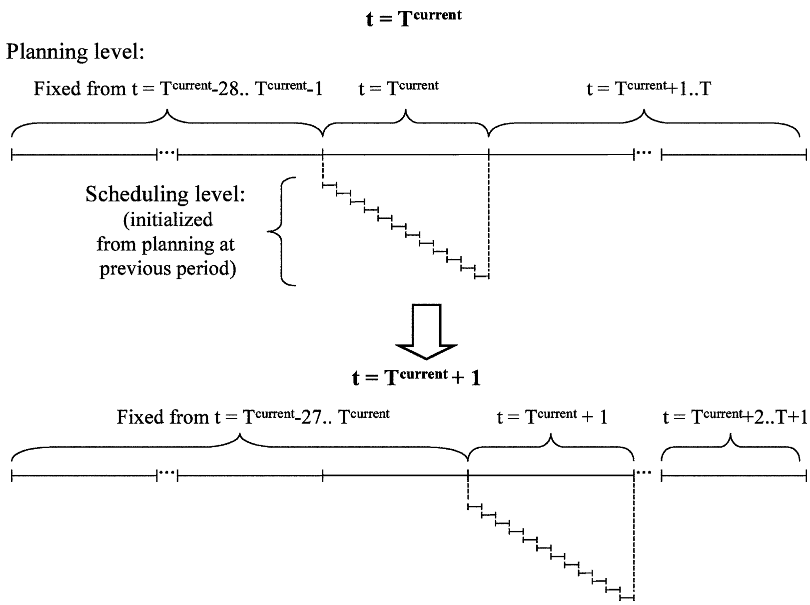

Fig. 3. Timeline representation for proposed methodology.

compressor operation in each scheduling period that adheres to the production and power targets from the planning level, while satisfying demands and pressure constraints. However, due to the nonlinearities on the scheduling level, a multiperiod solution might not be possible and an alternative is to solve each scheduling period in sequence and update the pipeline inventory at the end of each scheduling period. The scheduling level falls under the description 'reactive scheduling', seeing that the schedule is updated on an hourly basis as new measurements become available, regardless of whether the single period or multiperiod approach is used. In addition, the previous solve is used to initialize the current one, thus providing a good initial point for finding a feasible nonlinear solution. Future work could include a strategy for using the previous solve to reduce the search space for the current scheduling model, but this is not within the scope of this paper. We use the singe period approach in this work, but suspect that integration might be better facilitated with a multiperiod model. Before such a multiperiod model can be implemented, the nonlinearities at the scheduling level need to be addressed in depth in future work.

After the scheduling decisions for one planning period have been made, the initial inventory is updated for the next planning solution, and the demand forecast is updated based on any new demand information. In addition, the hydrogen production and power consumption resulting from the scheduling decisions are included as parameters for the next planning model to be considered in the price calculations. Fig. 3 shows the time representation for this strategy assuming sequential solution on the scheduling level.

The size of the scheduling model as implemented in this work, is independent of the number of time periods, since it is a single period model and only scales with the granularity of the pipeline calculations. The planning model, however, scales significantly with the number of time periods and the goal of 62 planning periods (1 month) leads to intractable solutions. To overcome this problem, we propose an approach where the planning is carried out for 2 weeks into the future, where production levels from the previous 2 weeks or more are used to complete a month horizon for the cost estimates. This past information is required, since a complete month of production and power consumption values are needed for the price calculations. Including 2 weeks of actual past information also gives more accuracy to this price calculation. We use a Lagrangean decomposition-based heuristic for the solution of the planning level.

4. Models

In this section, we present multiperiod MINLP optimization models for the production planning level and the reactive scheduling level. The scheduling model is presented as multiperiod for the sake of generality, although it is implemented as a single period model in this work due to the computational difficulty in solving this problem. Some constraints are applicable to both models and involve mainly the compressor description and the plant models. On the planning level, the complex price calculations are included while the pipeline model is approximated with an average pressure profile. In addition, the discrete decisions involving the hourly load steps are relaxed, and each compressor discharge pressure is fixed at its maximum value. On the scheduling level, the prices for feed and energy are fixed from the planning level, while the pipeline is modeled in detail, with varying pressures from compressor discharge to the customer. In addition, the discrete decisions involving plant on/off status are fixed, while the load step decisions are declared as binary variables (please refer to the nomenclature).

4.1. Multiperiod MINLP planning model

4.1.1. Compressor description

4.1.1.1. Load step calculations. The load step calculations in Eqs. (1)–(6) are valid for compressor k, at plant j, in pipelines l, as defined in the set $k^{\text{config}}(K,J,L)$ and planning periods $t \in T$, unless otherwise stated. The power used by the compressor (see Eq. (1)), is a function of the compressor efficiency, the suction pressure, the discharge pressure and a reference power that depends on the current load step as determined in Eq. (2). We assume the efficiency to be constant, the suction pressure is constant or variable depending on the compressor control structure (see Eq. (11)) and the discharge pressure is fixed to its maximum value for planning purposes (for scheduling purposes it is a variable).

$$\text{power}_{kjlt} = \text{power}^{\text{ref}}_{kjlt}\left(\frac{\eta_{kjlt}}{\eta^{\text{ref}}_{kjl}}\right)\left(\frac{P^{\text{suc}}_{kjlt}}{P^{\text{suc,ref}}_{kjl}}\right) \times \left[\frac{\left(\dfrac{P^{\text{dis,max}}_{kjlt}}{P^{\text{suc}}_{kjlt}}\right)^{(k^{\text{isen}}-1)/k^{\text{isen}}} - 1}{\left(\dfrac{P^{\text{dis,ref}}_{kjl}}{P^{\text{suc,ref}}_{kjl}}\right)^{(k^{\text{isen}}-1)/k^{\text{isen}}} - 1}\right] \tag{1}$$

$$\text{power}^{\text{ref}}_{kjlt} = \sum_a \text{power}^{\text{load}}_{akjlt} z_{akjlt} \tag{2}$$

The flow rate from the compressor (see Eq. (3)) is a function of the compressor efficiency, the suction pressure, the suction temperature and a reference flow rate that depends on the current load step as determined in Eq. (4). We assume a constant suction temperature.

$$\text{flow}_{kjlt} = \text{flow}^{\text{ref}}_{kjlt}\left(\frac{\eta_{kjlt}}{\eta^{\text{ref}}_{kjl}}\right)\left(\frac{P^{\text{suc}}_{kjlt}}{P^{\text{suc,ref}}_{kjl}}\right)\left[\frac{T^{\text{suc,ref}}_{kjl}}{T^{\text{suc}}_{kjlt}}\right] \tag{3}$$

$$\text{flow}^{\text{ref}}_{kjlt} = \sum_a \text{flow}^{\text{load}}_{akjlt} z_{akjlt} \tag{4}$$

Eq. (5) is a logical condition that states that each compressor must operate in exactly one load step. Adding an initial load step equal to 1 where the power and flow equals zero covers the case of no operation. Since the load step variables are relaxed between 0 and 1 for the planning model, these variables would then indicate the percentage of time the compressor can be expected to operate in each load step.

$$\sum_a z_{akjlt} = 1 \tag{5}$$

The degeneracy that may result from choosing between identical compressors is avoided by Eq. (6)

$$z_{akjlt} + \sum_{a'=a}^{A} z_{a'k'jlt} \le 1 \quad \forall a \in A,\ k,j,l \in k^{\text{config}}(K,J,L),\ k' \in \text{iden}^k(K,K'),\ t \in T \tag{6}$$

which specifies that the load step of the first compressor should always be greater or equal to the second if both are in operation.

4.1.1.2. Other compressor calculations. Each compressor has one of two control structures, the first controlling the flow rate through recycle with a fixed suction pressure and the second controlling flow rate with a combination of recycle and a throttle on the suction side, i.e. variable suction pressure. Eqs. (7)–(10) are valid for both control structures and Eq. (11) is specific to the second control structure. Furthermore, constraints Eqs. (7)–(11) are valid for all $k,j,l \in k^{\text{config}}(K,J,L)$ and $t \in T$, unless otherwise stated. The flow rate exiting the compressor into the pipeline is the difference between the compressor flow rate and the recycle flow rate:

$$\text{flow}^{\text{comp}}_{kjlt} = \text{flow}_{kjlt} - \text{flow}^{\text{recy}}_{kjlt} \tag{7}$$

Bounds on the compressor and recycle flow rates are enforced by Eq. (8) and Eq. (9) if the compressor is in operation,

$$L^{\text{flow}}_{kjl}\sum_{a=2}^{A} z_{akjlt} \le \text{flow}_{kjlt} \le U^{\text{flow}}_{kjl}\sum_{a=2}^{A} z_{akjlt} \tag{8}$$

$$0 \le \text{flow}^{\text{recy}}_{kjlt} \le U^{\text{flow},r}_{kjl}\sum_{a=2}^{A} z_{akjlt} \tag{9}$$

while the logical condition in Eq. (10) specifies that a compressor can only operate if the associated plant j operates at time period t.

$$\sum_{a=2}^{A} z_{akjlt} \le y_{j,t} \tag{10}$$

For control structure 2, the suction throttle is calculated in Eq. (11) as the difference between the feed pressure and suction pressure.

$$P^{\text{suc}}_{kjlt} = P^{\text{feed}}_{kjl} - \Delta P^{\text{suc}}_{kjlt} \quad \forall k,j,l \in k^{\text{config}}(K,J,L) \cap c^2(K,J,L),\ t \in T \tag{11}$$

4.1.2. Constraints general to all plants

Consider the following constraints that are valid for each plant $j \in J$, with validity over additional indices where stated. Eq. (12) is only enforced if a compressor exists in pipeline l and specifies that the total flow rate into pipeline l from plant j in period t equals the sum of flow rates from the compressors discharging into pipeline l from plant j.

$$\text{pipeflow}_{jlt} = \sum_{k \in k^{\text{config}}(K,J,L)} \text{flow}^{\text{comp}}_{kjlt} \quad \forall l \in H2L(L),\ t \in T \tag{12}$$

The total hydrogen flow rate from plant j in period t equals the sum of the flow rates to different pipelines, as indicated by Eq. (13).

$$\text{H}_2\text{flow}_{jt} = \sum_{l \in H2L(L)} \text{pipeflow}_{jlt} \quad \forall t \in T \tag{13}$$

Lower and upper bounds on the total hydrogen flow rate are enforced if the plant is in operation through Eq. (14).

$$L_j^{\text{H}_2\text{flow}} y_{jt} \le \text{H}_2\text{flow}_{jt} \le U_j^{\text{H}_2\text{flow}} y_{jt} \quad \forall t \in T \tag{14}$$

The total power consumed by plant j in period t is the sum of the power from all the associated compressors and the auxiliary power, and is given by the following constraint

$$\text{plantpower}_{jt} = \text{auxpower}_{jt} + \sum_{k,l \in k\_\text{config}(K,J,L)} \text{power}_{kjlt} \quad \forall t \in T \tag{15}$$

while the auxiliary power is defined in Eq. (16) as a function of the hydrogen flow rate.

$$\text{auxpower}_{jt} = \text{aux}_j^1 y_{jt} + \text{aux}_j^2(\text{H}_2\text{flow}_{jt} - \text{aux}_j^3 y_{jt}) \quad \forall t \in T \tag{16}$$

The total hydrogen production for each plant over the whole planning horizon is calculated in Eq. (17) and will be used later in the price calculations.

$$\text{H}_2\text{flow}_j^{\text{tot}} = \sum_t \text{H}_2\text{flow}_{jt}\text{duration}_t \tag{17}$$

Logical conditions are enforced by Eq. (18) and Eq. (19), namely that a plant can only operate if it is ‘on’ during the planning horizon and the plant is ‘off’ if it does not operate in any time period.

$$y_j^{\text{on}} \ge y_{jt} \quad \forall t \in T \tag{18}$$

$$y_j^{\text{on}} \le \sum_t y_{j,t} \tag{19}$$

4.1.3. Constraints specific to offgas plants

Fig. 4 shows a typical configuration for an offgas plant, and represents the structure used for plants 1, 2 and 5. Each plant can have connections to one or more pressure levels, and can have single or parallel compressors in each line.

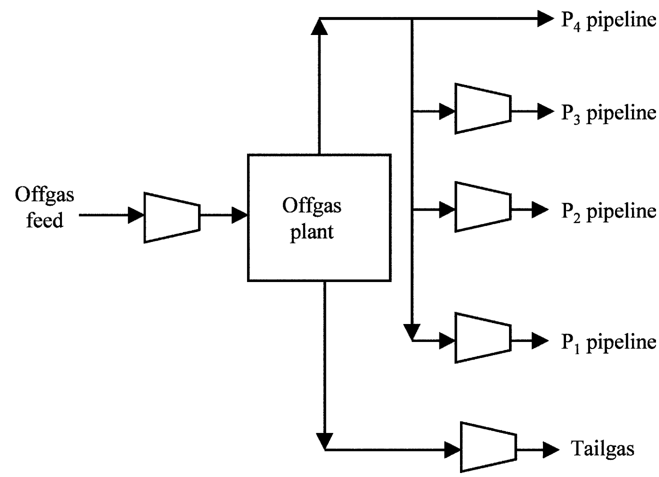

Fig. 4. Typical structure for offgas plants.

Eqs. (20)–(25) are valid for all $j \in \text{OG}(J)$ and $t \in T$, while Eqs. (26), (27), (28a) and (29) are valid for all $j \in \text{OG}(J)$. Eq. (20) and Eq. (21) are only enforced if compressors exist in the offgas and tailgas pipelines, respectively and calculate the offgas and tailgas flow rates as the sums of the respective compressor flow rates.

$$\text{ogflow}_{jt} = \sum_{k \in k^{\text{config}}(K,\text{OG},\text{OGL})} \text{flow}^{\text{comp}}_{k,j,\text{ogl},t} \tag{20}$$

$$\text{tgflow}_{jt} = \sum_{k \in k^{\text{config}}(K,\text{OG},\text{TGL})} \text{flow}^{\text{comp}}_{k,j,\text{tgl},t} \tag{21}$$

The mass balance across the plant is given by Eq. (22) and the hydrogen flow rate is a function of the offgas flow rate, the hydrogen composition in the feed to the plant and the hydrogen recovery as stated in Eq. (23).

$$\text{tgflow}_{jt} = \text{ogflow}_{jt} - \text{H}_2\text{flow}_{jt} \tag{22}$$

$$\text{H}_2\text{flow}_{jt} = \text{ogflow}_{jt}(0.01\ \ H_{2j}^{\text{og,comp}}\text{H}_2\text{recov}_{jt}) \tag{23}$$

Below a pre-specified intermediate level of hydrogen production, H_2inter, the hydrogen recovery is a function of the hydrogen flow rate given on the right hand side (RHS) of Eq. (24). Above this intermediate level, the recovery is equal to the constant RHS of Eq. (25). This relationship is strictly enforced by the inequalities Eq. (24) and Eq. (25), since the RHS of Eq. (24) will always be smaller than the RHS of Eq. (25) for hydrogen flow rates less than the intermediate value.

$$\text{H}_2\text{recov}_{jt} \le 100 - c_j^{\text{recov}}\left(\frac{\text{H}_2\text{inter}_j}{\text{H}_2\text{flow}_{jt}}\right) \tag{24}$$

$$\text{H}_2\text{recov}_{jt} \le 100 - c_j^{\text{recov}} \tag{25}$$

For the offgas plants, the feedcost is a function of the offgas price and the total hydrogen production during the whole planning horizon:

$$\text{feedcost}_j = \text{ogprice}_j \text{H}_2\text{flow}_j^{\text{tot}} \text{H}_2\text{purity}_j \tag{26}$$

A constant offgas multiplier, a variable natural gas multiplier and a constant natural gas price determine the offgas price as follows

$$\text{ogprice}_j = \text{OGM}_j \text{NGM}_j c_j^{\text{ngprice}} \tag{27}$$

The natural gas multiplier is a function of the amount of hydrogen supplied to the offgas provider, as well as the total hydrogen produced during the whole planning horizon and is modeled through disjunction Eq. (28a) and Eq. (28b). In this disjunction, the OR sign ($\vee$), indicates that either the left group of constraints are true ($b_j^{1,\text{NGM}}$ = True) in which case Eq. (28a) determines the natural gas multiplier, NGM_j, or the right group of constraints are true ($b_j^{2,\text{NGM}}$ = True) in which case Eq. (28b) determines the multiplier. Disjunction Eq. (28a) and Eq. (28b) and all other disjunctive constraints that will be shown further on in the model are eventually converted to mixed integer form by using the convex hull formulation. These derivations are not shown here, but we refer the interested reader to Balas (1985) and Türkay and Grossmann (1996).

$$\begin{bmatrix} b_j^{1,\text{NGM}} \\ \text{H}_2\text{ogpro}_j \le \text{H}_2\text{flow}_j^{\text{tot}} \le \text{H}_{2j}^{\min} \sum_t \text{duration}_t + \text{H}_2\text{ogpro}_j \\ \text{NGM}_j = a_j^{\text{NGM}} \left(\dfrac{\text{H}_2\text{flow}_j^{\text{tot}} - \text{H}_2\text{ogpro}_j}{\text{H}_2\text{flow}_j^{\text{tot}}} \right) \qquad (28\text{a}) \end{bmatrix}$$

$$\vee \begin{bmatrix} b_j^{2,\text{NGM}} \\ \text{H}_{2j}^{\min} \sum_t \text{duration}_t + \text{H}_2\text{ogpro}_j \le \text{H}_2\text{flow}_j^{\text{tot}} \le \text{H}_{2j}^{\max} \sum_t \text{duration}_t + \text{H}_2\text{ogpro}_j \\ \text{NGM}_j = b_j^{\text{NGM}} \left(\dfrac{\text{H}_2\text{flow}_j^{\text{tot}} - \text{H}_2\text{ogpro}_j}{\text{H}_2\text{flow}_j^{\text{tot}}} \right) + (a_j^{\text{NGM}} - b_j^{\text{NGM}}) \left(\dfrac{\text{H}_{2j}^{\min} \sum_t \text{duration}_t}{\text{H}_2\text{flow}_j^{\text{tot}}} \right) \qquad (28\text{b}) \end{bmatrix} \quad \forall j \in OG(J) \tag{28}$$

The logical condition in Eq. (29) specifies that if plant j operates during the planning horizon, exactly one of the sets of constraints from disjunction Eq. (28a) or Eq. (28b) are valid. Otherwise, if plant j does not operate at all during the planning horizon, neither of the constraint sets will be considered and the feed cost would be zero.

$$b_j^{1,\text{NGM}} + b_j^{2,\text{NGM}} = y_j^{\text{on}} \tag{29}$$

The problem of division by zero that may arise if the total flow is zero, is avoided by some algebraic manipulations and substitutions of constraints Eqs. (26), (27), (28a) and (28b).

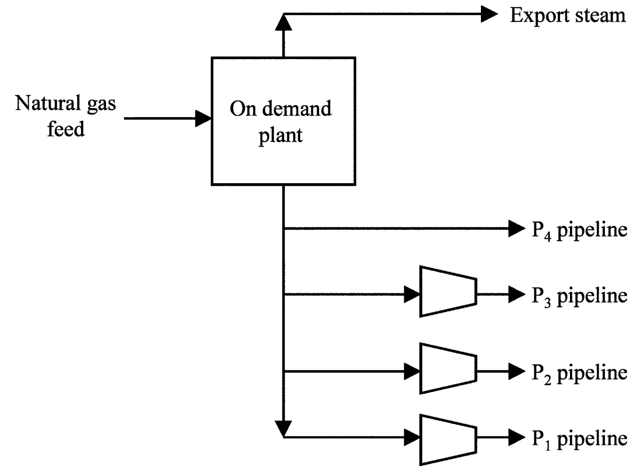

Fig. 5. Typical structure for on-demand plants.

4.1.4. Constraints specific to 'on-demand' plants

Fig. 5 shows a superstructure for a typical 'on-demand' plant and is the structure used for plants 3 and 4. Each plant can have connections to one of more pressure levels, and can have single or parallel compressors in each line.

Of these two plants, only plant 3 is truly 'on-demand', and it exports steam to generate revenue. Hydrogen is a co-product from plant 4, whose production rate is determined by the demand for the other product. Thus, for the purpose of this study, the hydrogen production rate from plant 4 will be fixed. The pricing calculations (see disjunction Eqs. (33a), (33b) and (33c) and Eq. (33d)) need therefore only be carried out for plant 3, while plant 4 has a fixed natural gas price. The on-demand plant constraints Eqs. (30)–(32), (33a), (33b), (33c), (33d), (34)–(39) are valid for all $j \in$ OD(J) with additional domains where indicated.

The natural gas flow rate is related to the hydrogen flow rate through a third order polynomial function given in Eq. (30),

$$\mathrm{ngflow}_{jt} = a_{0j}y_{jt} + a_{1j}\mathrm{H_2flow}_{jt} + a_{2j}\mathrm{H_2flow}_{jt}^2 + a_{3j}\mathrm{H_2flow}_{jt}^3 \quad \forall t \in T \tag{30}$$

and the total natural gas flow during the whole planning horizon is calculated in Eq. (31).

$$\mathrm{ngflow}_j^{\mathrm{tot}} = \sum_t \mathrm{ngflow}_{jt}\mathrm{duration}_t \tag{31}$$

Total feed cost for plant j is the product of the natural gas price and the total natural gas flow for the whole planning horizon:

$$\mathrm{feedcost}_j = \mathrm{ngprice}_j \mathrm{ngflow}_j^{\mathrm{tot}} \tag{32}$$

For the on-demand plants, the natural gas price is a variable that depends on the total natural gas flow and is determined by the following disjunction:

In this case, the disjunction has five possible outcomes as specified by the logical Eq. (34):

$$b_j^{1,\mathrm{NGPrice}} + b_j^{2,\mathrm{NGPrice}} + b_j^{3,\mathrm{NGPrice}} + b_j^{4,\mathrm{NGPrice}} = y_j^{\mathrm{on}} \tag{34}$$

If plant j does not operate at all, then none of the disjunctive terms are considered and the feed cost is set to zero, otherwise, if plant j does operate, exactly one of the four disjunctive terms must hold. Certain pre-set bounds determine four intervals that indicate which of the disjunctive sets are valid. For example, if the total natural gas flow is below $\mathrm{ngflow1}_j$, then $b_j^{1,\mathrm{NGPrice}} =$ True and the natural gas price is determined by Eq. (33a). Again, the problem that may arise from division by zero if the natural gas flow is zero, is avoided by some algebraic manipulations and substitutions.

$$\begin{bmatrix} b_j^{1,\mathrm{NGPrice}} \\ 0 \le \mathrm{ngflow}_j^{\mathrm{tot}} \le \mathrm{ngflow1}_j \\ \mathrm{ngprice}_j = \mathrm{FERC}_j + \Delta\mathrm{FERC1}_j \end{bmatrix} \tag{33a}$$

$$\vee \begin{bmatrix} b_j^{2,\mathrm{NGPrice}} \\ \mathrm{ngflow1}_j \le \mathrm{ngflow}_j^{\mathrm{tot}} \le \mathrm{ngflow2}_j \\ \mathrm{ngprice}_j = \dfrac{\mathrm{ngflow1}_j}{\mathrm{ngflow}_j^{\mathrm{tot}}}(\mathrm{FERC}_j + \Delta\mathrm{FERC1}_j) + \left(1 - \dfrac{\mathrm{ngflow1}_j}{\mathrm{ngflow}_j^{\mathrm{tot}}}\right)(\mathrm{FERC}_j + \Delta\mathrm{FERC2}_j) \end{bmatrix} \tag{33b}$$

$$\vee \begin{bmatrix} b_j^{3,\mathrm{NGPrice}} \\ \mathrm{ngflow2}_j \le \mathrm{ngflow}_j^{\mathrm{tot}} \le \mathrm{ngflow3}_j \\ \mathrm{ngprice}_j = \dfrac{\mathrm{ngflow1}_j}{\mathrm{ngflow}_j^{\mathrm{tot}}}(\mathrm{FERC}_j + \Delta\mathrm{FERC1}_j) + \left(\dfrac{\mathrm{ngflow2}_j - \mathrm{ngflow1}_j}{\mathrm{ngflow}_j^{\mathrm{tot}}}\right) \\ \quad \times(\mathrm{FERC}_j + \Delta\mathrm{FERC2}_j) + \left(1 - \dfrac{\mathrm{ngflow2}_j}{\mathrm{ngflow}_j^{\mathrm{tot}}}\right)(\mathrm{FERC}_j + \Delta\mathrm{FERC3}_j) \end{bmatrix} \tag{33c}$$

$$\vee \begin{bmatrix} b_j^{4,\mathrm{NGPrice}} \\ \mathrm{ngflow3}_j \le \mathrm{ngflow}_j^{\mathrm{tot}} \\ \mathrm{ngprice}_j = \dfrac{\mathrm{ngflow1}_j}{\mathrm{ngflow}_j^{\mathrm{tot}}}(\mathrm{FERC}_j + \Delta\mathrm{FERC1}_j) + \left(\dfrac{\mathrm{ngflow2}_j - \mathrm{ngflow1}_j}{\mathrm{ngflow}_j^{\mathrm{tot}}}\right) \\ \quad \times(\mathrm{FERC}_j + \Delta\mathrm{FERC2}_j) + \left(\dfrac{\mathrm{ngflow3}_j - \mathrm{ngflow2}_j}{\mathrm{ngflow}_j^{\mathrm{tot}}}\right)(\mathrm{FERC}_j + \Delta\mathrm{FERC3}_j) \\ \quad + \left(1 - \dfrac{\mathrm{ngflow3}_j}{\mathrm{ngflow}_j^{\mathrm{tot}}}\right)(\mathrm{FERC}_j + \Delta\mathrm{FERC4}_j) \end{bmatrix} \tag{33d}$$

The steam flow rate from the on-demand plants is a quadratic function of the hydrogen flow rate as shown in the following constraint:

$$\mathrm{steamflow}_{jt} = (a_{0j}y_{jt} + a_{1j}\mathrm{H_2flow}_{jt} + a_{2j}\mathrm{H_2flow}_{jt}^2)/c_j^{\mathrm{steam}} \quad \forall t \in T \tag{35}$$

Steam generated by the on-demand plants can possibly be exported to generate revenue, but only up to a certain amount of steam, $U_j^{st,\exp}$, and any steam above this value will be vented with no added benefit as denoted by Eq. (36) and Eq. (37).

$$\mathrm{steamflow}_{jt} = \mathrm{steamexp}_{jt} + \mathrm{steamvent}_{jt} \tag{36}$$

$$\mathrm{steamexp}_{jt} \le U_j^{st,\exp} y_{jt} \quad \forall t \in T \tag{37}$$

The steam revenue for each period is then the product of the exported steam and the steam credit,

$$\mathrm{steamrev}_{jt} = \mathrm{steamcred}_j \mathrm{steamexp}_{jt} \mathrm{duration}_t \quad \forall t \in T \tag{38}$$

where the steam credit is a function of the natural gas price and some index values:

$$\mathrm{steamcred}_j = (1-\alpha_j^{\mathrm{steam}})\mathrm{ngprice}_j + \alpha_j^{\mathrm{steam}}\left(\frac{\mathrm{ECI}_j}{\mathrm{ECI}_j^{\mathrm{ref}}}\right) \tag{39}$$

4.1.5. Energy cost calculations general to all plants

The energy cost for each plant is determined by the average power consumption for each plant over the whole planning horizon, as well as from the averages of the N^{peak} highest off- and on-peak power consumption, respectively. To this end, we define that the hours between 08:00 a.m. and 08:00 p.m. are on-peak, while the remainder are off-peak, i.e. every second time period is off-peak. Eqs. (40)–(47), (48a), (49a), (50) and (51) are valid for all plants $j \in J$ with additional domains where indicated. Eq. (40) shows the calculation of the energy cost for each plant j($\mathrm{powercost}_j$) to be a constant base price plus a variable price, multiplied by the total power consumption.

$$\mathrm{powercost}_j = c_j^{\mathrm{base}} \sum_t \mathrm{plantpower}_{jt}\mathrm{duration}_t + \left[\frac{(c_j^{\mathrm{prim}}\mathrm{primKWHR}_j + c_j^{\mathrm{scnd}}\mathrm{scndKWHR}_j)}{\mathrm{avgpower}_j 24 \text{ days}}\right] \times \sum_t \mathrm{plantpower}_{jt}\mathrm{duration}_t \tag{40}$$

The variable price component involves three variable components, namely a primary and secondary value for kWh of power and the average power consumption over all periods. Of these, the average power consumption involves the simplest calculation as shown in Eq. (41), where $|T|$ indicates the cardinality of the set T.

$$\mathrm{avgpower}_j = \frac{\sum_{t\in T} \mathrm{plantpower}_{jt}}{|T|} \tag{41}$$

The calculations of the other two variable terms are more involved and are described in constraints Eqs. (42)–(47), (48a), (49a), (50) and (51), all of which are valid for all plants $j \in J$, with additional domains where indicated. First, the average of the N^{peak} highest on- and off-peak power consumption for all planning periods need to be determined to calculate a monthly on-peak average and a monthly off-peak average as shown in Eq. (42) and Eq. (43), where $|N^{\mathrm{peak}}|$ indicates the cardinality of the set N^{peak}.

$$\mathrm{mo}_j^{\mathrm{on}} = \frac{\sum_{n^{\mathrm{peak}}} \max^{\mathrm{on}}_{n^{\mathrm{peak}},j}}{|N^{\mathrm{peak}}|} \tag{42}$$

$$\mathrm{mo}_j^{\mathrm{off}} = \frac{\sum_{n^{\mathrm{peak}}} \max^{\mathrm{off}}_{n^{\mathrm{peak}},j}}{|N^{\mathrm{peak}}|} \tag{43}$$

Modeling the determination of the N^{peak} largest peaks is not obvious, since these are variables and it is not known beforehand which will be the largest. One option is to enumerate all possible combinations, but this will become combinatorially explosive. Instead we use the following big-M formulation, where $|T^{\mathrm{on}}|$ represents the cardinality of the set T^{on}, shown for the calculation of the on-peak maximum (it is similar for the off-peak calculation). Consider Eqs. (44)–(47) as they relate to determining the largest peak, with the order of n^{peak} therefore being equal to 1. Eq. (44) and Eq. (45) imply that the first largest peak for plant j must be greater or equal to the power consumption for all on-peak periods. This can be seen from the RHS of Eq. (45), which equals $|T^{\mathrm{on}}|$. In addition, Eq. (46) and Eq. (47) imply that the first largest peak must be less or equal to exactly 1 period's power consumption, as enforced by the RHS of Eq. (47). Similarly, the second largest peak must be greater or equal to exactly $|T^{\mathrm{on}}|-1$ peaks and less or equal to exactly two peaks and so forth.

$$\max^{\mathrm{on}}_{n^{\mathrm{peak}},j} \geq \mathrm{plantpower}_{jt\_\mathrm{on}} c^{\mathrm{power\_cost}} - U(1 - b^{1,\mathrm{onpeak}}_{j,n^{\mathrm{peak}},t\_\mathrm{on}}) \quad \forall n^{\mathrm{peak}} \in N^{\mathrm{peak}}, \quad t\_\mathrm{on} \in T^P \tag{44}$$

$$\sum_{t\_\mathrm{on}} b^{1,\mathrm{onpeak}}_{j,n^{\mathrm{peak}},t\_\mathrm{on}} = |T^{\mathrm{on}}| - n^{\mathrm{peak}} + 1 \quad \forall n^{\mathrm{peak}} \in N^{\mathrm{peak}} \tag{45}$$

$$\max^{\mathrm{on}}_{n^{\mathrm{peak}},j} \leq \mathrm{plantpower}_{jt\_\mathrm{on}} c^{\mathrm{power\_cost}} + U(1 - b^{2,\mathrm{onpeak}}_{j,n^{\mathrm{peak}},t\_\mathrm{on}}) \quad \forall n^{\mathrm{peak}} \in N^{\mathrm{peak}}, \quad t\_\mathrm{on} \in T^P \tag{46}$$

$$\sum_{t\_\mathrm{on}} b^{2,\mathrm{onpeak}}_{j,n^{\mathrm{peak}},t\_\mathrm{on}} = n^{\mathrm{peak}} \quad \forall n^{\mathrm{peak}} \in N^{\mathrm{peak}} \tag{47}$$

The logical propositions in Eq. (48a) and Eq. (48b) are added to this big-M formulation, where Eq. (48a) implies that if constraint Eq. (44) is not enforced for the n^{peak} largest peak in t_on, then Eq. (46) must be enforced. In other words, Eq. (48a) implies that if a peak value is not greater than or equal to a certain power level, then it must be less than that power level. Similarly, Eq. (48b) implies that if a peak value is not less than or equal to a certain power level, then it must be greater than that power level. The converse is not true, i.e. if the peak level is reater or equal to a certain power level and Eq. (44), it can either be equal, in which case Eq. (46) will also be enforced for that instance, or it can be strictly greater, in which case Eq. (46) will not be enforced and thus no logic can be given for the converse case.

$$\neg\, b^{1,\mathrm{onpeak}}_{j,n^{\mathrm{peak}},t\_\mathrm{on}} \Rightarrow b^{2,\mathrm{onpeak}}_{j,n^{\mathrm{peak}},t\_\mathrm{on}} \quad \forall n^{\mathrm{peak}} \in N^{\mathrm{peak}}, \quad t\_\mathrm{on} \in T^P \tag{48a}$$

$$\neg b^{2,\text{onpeak}}_{j,n^{\text{peak}},t\_\text{on}} \Rightarrow b^{1,\text{onpeak}}_{j,n^{\text{peak}},t\_\text{on}} \quad \forall n^{\text{peak}} \in N^{\text{peak}},\ \ t\_\text{on} \in T^{P} \tag{48b}$$

These logic propositions are converted into the integer Eq. (48c). Similar constraints are added for the off-peak formulation. These logic constraints are redundant, but help to reduce the size of the branch and bound tree.

$$b^{1,\text{onpeak}}_{j,n^{\text{peak}},t\_\text{on}} + b^{2,\text{onpeak}}_{j,n^{\text{peak}},t\_\text{on}} \geq 1 \quad \forall n^{\text{peak}} \in N^{\text{peak}},\ \ t\_\text{on} \in T^{P} \tag{48c}$$

Next, the values for mo_j^{on} and mo_j^{off} are used in disjunction Eqs. (49a), (49b) and (49c) to calculate the value of primKVA_j, a measure for the eventual price calculations. If the monthly on-peak average is greater than the monthly off-peak average, the first part of the disjunction is valid and primKVA_j is calculated according to Eq. (49a). Otherwise, if the monthly on-peak average is less than the monthly off-peak average **and** the monthly off-peak average is less than the annual on-peak average, the second part of the disjunction is valid and primKVA_j is calculated according to Eq. (49b). Otherwise, if the monthly on-peak average is less than the monthly off-peak average **and** the monthly off-peak average is greater than the annual on-peak average, the third part of the disjunction is valid and primKVA_j is set equal to the annual on-peak average according to constraint Eq. (49c).

$$\begin{bmatrix} b_j^{1,\text{pKVA}} \\ \text{mo}_j^{\text{on}} \geq \text{mo}_j^{\text{off}} \\ \text{primKVA}_j = \max\begin{bmatrix} \text{mo}_j^{\text{on}} \\ \text{peakfrac}_j\text{annon}_j \\ \min_j^{\text{pKVA}} \end{bmatrix} \ (49\text{a}) \end{bmatrix} \vee \begin{bmatrix} b_j^{2,\text{pKVA}} \\ \text{mo}_j^{\text{on}} \leq \text{mo}_j^{\text{off}} \\ \text{mo}_j^{\text{off}} \leq \text{annon}_j \\ \text{primKVA}_j = \max\begin{bmatrix} \text{mo}_j^{\text{off}} \\ \text{peakfrac}_j\text{annon}_j \\ \min_j^{\text{pKVA}} \end{bmatrix} \ (49\text{b}) \end{bmatrix} \vee \begin{bmatrix} b_j^{3,\text{pKVA}} \\ \text{mo}_j^{\text{on}} \leq \text{mo}_j^{\text{off}} \\ \text{mo}_j^{\text{off}} \geq \text{annon}_j \\ \text{primKVA}_j = \text{annon}_j \end{bmatrix} (49\text{c}) \tag{49}$$

Eq. (49a) and Eq. (49b) are max functions, which need to be reformulated to avoid discontinuities. A common mixed-integer reformulation is shown below for Eq. (49a) in the first part of the disjunction and is similar for other max or min functions where required. Eq. (49a).1, Eq. (49a).2, Eq. (49a).3 state that the primKVA_j must be greater than or equal to all three of the values inside the max function. However, it must also be equal to exactly one of these values, and this is enforced by constraints Eq. (49a).4 through Eq. (49a).7, since the equality is not automatically satisfied in the optimization.

$$\begin{bmatrix} b_j^{1,\text{pKVA}} & \\ \text{mo}_j^{\text{on}} \geq \text{mo}_j^{\text{off}} & \\ \text{primKVA}_j \geq \text{mo}_j^{\text{on}} & (49\text{a}.1) \\ \text{primKVA}_j \geq \text{peakfrac}_j\text{annon}_j & (49\text{a}.2) \\ \text{primKVA}_j \geq \min_j^{\text{pKVA}} & (49\text{a}.3) \\ \text{primKVA}_j \leq \text{mo}_j^{\text{on}} + U(1 - b_j^{1,\max}) & (49\text{a}.4) \\ \text{primKVA}_j \leq \text{peakfrac}_j\text{annon}_j + U(1 - b_j^{2,\max}) & (49\text{a}.5) \\ \text{primKVA}_j \leq \min_j^{\text{pKVA}} + U(1 - b_j^{3,\max}) & (49\text{a}.6) \\ b_j^{1,\max} + b_j^{2,\max} + b_j^{3,\max} = 1 & (49\text{a}.7) \end{bmatrix}$$

Eventually, the value of primKVA_j is then used in Eq. (50) and Eq. (51) to calculate the primary and secondary values for kWh of power to be used in the final energy cost calculation given by constraint Eq. (40). Eq. (50) specifies that the primary value is the minimum of the average power converted to a monthly value, and the primKVA_j also converted with the constant $c^{\text{power\_cost}}$. The min function is reformulated similar to Eq. (49a) above.

$$\text{primKWHR}_j = \min\begin{bmatrix} 24(30)(\text{avgpower}_j) \\ c^{\text{powercost}}\text{primKVA}_j \end{bmatrix} \tag{50}$$

Eq. (51) specifies that the secondary value is the maximum of zero and the difference between the average power and primKVA_j, both converted to monthly values.

$$\text{scndKWHR}_j = \max\begin{bmatrix} 0 \\ 24(30)(\text{avgpower}_j) - c^{\text{powercost}}\text{primKVA}_j \end{bmatrix} \tag{51}$$

In this case the max function can be represented by two 'greater than or equal to' inequalities (Eq. (51a) and Eq. (51b)), since equality will be enforced by the objective that minimizes scndKWHR_j:

$$\text{scndKWHR}_j \geq 0 \tag{51a}$$

$$\text{scndKWHR}_j \geq 24(30)(\text{avgpower}_j) - c^{\text{powercost}}\text{primKVA}_j \tag{51b}$$

4.1.6. Pipeline model

For the planning level, the pipeline model is simplified since the length of each planning period is 12 h and it is therefore reasonable to use an average pressure for each pressure level in each time period. For both the planning and scheduling models, the pipeline is divided into shorter sections and modeled as a network of nodes and arcs. Fig. 6 shows a small example of such a network, where artificial nodes have been added to the

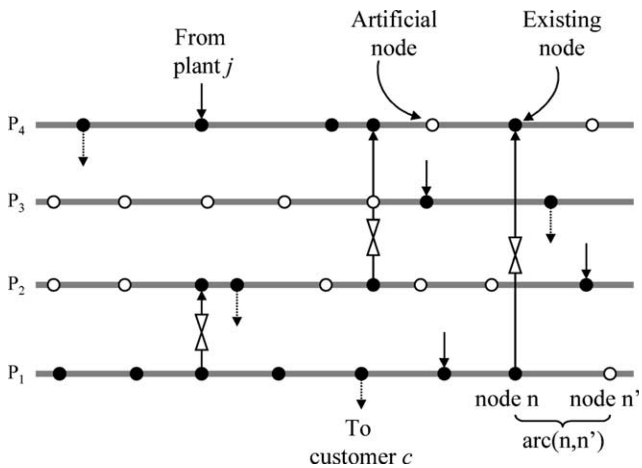

Fig. 6. Pipeline network of nodes and arcs.

existing nodes to get a more accurate model of the inventory in the pipeline. An arc is defined between any two nodes n and n'.

Eqs. (52)–(55) are valid for all $n \in N$ and $t \in T$, unless stated otherwise. From Fig. 6 it is clear that a node can receive hydrogen from another node or from a plant, and send hydrogen to another node or to a customer. This is depicted in the mass balance for each node given by Eq. (52).

$$\begin{aligned}\mathrm{inv}_{n,t} = {} & \mathrm{inv}_{n,t-1} \\ & + \Bigg(\mathrm{plantflow}_{n,t} + \sum_{n' \in \mathrm{arc}(n',n)} \mathrm{flowarc}_{n',n,t} \\ & - \mathrm{custflow}_{n,t} - \sum_{n' \in \mathrm{arc}(n,n')} \mathrm{flowarc}_{n,n',t}\Bigg)\mathrm{duration}_t\end{aligned} \tag{52}$$

This constraint states that the inventory associated with node n in the current period, equals the inventory in the previous period plus the resultant of all flow rates in or out, multiplied by the duration of the time period. The plant flow into each node equals the flow from the associated plant as calculated in Eq. (53)

$$\mathrm{plantflow}_{n,t} = \sum_{\substack{j \in \\ p\_\mathrm{node}(j,n)}} \sum_{\substack{l \in \\ n\_\mathrm{pipe}(h2l,n)}} \mathrm{pipeflow}_{j,h2l,t} \tag{53}$$

while the customer flow from each node equals the flow to the associated customer as calculated in Eq. (54). The assumption here is that the demand should be satisfied exactly.

$$\mathrm{custflow}_{n,t} = \sum_{\substack{c \in \\ c\_\mathrm{node}(c,n)}} \sum_{\substack{l \in \\ n\_\mathrm{pipe}(h2l,n)}} \mathrm{custdem}_{j,h2l,t} \tag{54}$$

To model the inventory, we assign to each node the inventory of one half of each arc connected to it as shown in Eq. (55). The other half is assigned to the node on the other end of the arc. In this constraint, inventory is estimated as the average density multiplied by the volume of half of the arcs connected to it. Bounds are set on the average pressure to ensure realistic values for this variable. The accuracy of Eq. (55) depends highly on the granularity of the pipeline arc-sections, and to account for errors, the positive slack variables $s1^{\mathrm{inv}}$ and $s2^{\mathrm{inv}}$ are added. These slacks are minimized in the objective function Eq. (56) with an appropriate weight to drive them to zero. In fact, while these slacks are essential to determine an initial feasible solution, we found that they are eventually driven to zero for the planning level.

$$\begin{aligned}\mathrm{inv}_{n,t} = \frac{\pi}{8}\Bigg[& \sum_{\substack{n' \in [\mathrm{arc}(n,n') \\ \cap n\_\mathrm{pipe}(h2l,n')]}} \frac{D^2_{n,n'} L_{n,n'} (P^{\mathrm{avg}}_{h2l,t})}{R_g T_{\mathrm{abs}}} + \\ & \sum_{\substack{n' \in [\mathrm{arc}(n',n) \\ \cap n\_\mathrm{pipe}(h2l,n')]}} \frac{D^2_{n,n'} L_{n',n} (P^{\mathrm{avg}}_{h2l,t})}{R_g T_{\mathrm{abs}}}\Bigg] + s1^{\mathrm{inv}}_{n,t} - s2^{\mathrm{inv}}_{n,t}\end{aligned} \tag{55}$$

$$\forall (n, h2l) \in n\_\mathrm{pipe}(h2l, n), \quad t \in T$$

4.1.7. Objective

The objective of the planning level is to minimize costs over the whole planning horizon, and includes power costs, feed costs and steam revenues for all the plants, as well as the slacks from the inventory constraints multiplied by a sufficiently large weight:

$$\begin{aligned}\min Z = & \sum_j \left(\mathrm{powercost}_j + \mathrm{feedcost}_j - \sum_t \mathrm{steamrev}_{jt}\right) \\ & + \sum_n \sum_t w^{\mathrm{inv}} (s1^{\mathrm{inv}}_{n,t} + s2^{\mathrm{inv}}_{n,t})\end{aligned} \tag{56}$$

In addition, lower and upper bounds are specified for all variables, but not shown here.

4.2. MINLP scheduling model

Since there is significant overlap between the planning model and the scheduling model, we will only write out the constraints that change or are added for scheduling and mention the overlapping constraints by number. For the scheduling model, the y variables are fixed, indicated by $\bar{y}$, while the z variables are declared as binary. In addition, prices are fixed where indicated and all binary variables associated with the cost calculations are therefore excluded. For the sake of generality, we present the model as a multiperiod model, but it should be understood that for the purpose of this work there is only one time period with length 1 h, solved sequentially for 12 h-long periods after which the production plan is updated.

4.2.1. Compressor description

The compressor constraints for reactive scheduling are the same as Eq. (1) through Eq. (11) from the planning model, except that Eq. (1) now includes a variable discharge pressure for each compressor instead of the maximum pressure, as shown in the updated Eq. (57), with validity the same as for Eq. (1).

$$\mathrm{power}_{kjlt} = \mathrm{power\_ref}_{kjlt}\left(\frac{\eta_{kjlt}}{\eta^{\mathrm{ref}}_{kjl}}\right)\left(\frac{P^{\mathrm{suc}}_{kjlt}}{P^{\mathrm{suc,ref}}_{kjl}}\right) \times \left[\frac{\left(\frac{P^{\mathrm{dis}}_{kjlt}}{P^{\mathrm{suc}}_{kjlt}}\right)^{(k^{\mathrm{isen}}-1)/k^{\mathrm{isen}}} - 1}{\left(\frac{P^{\mathrm{dis,ref}}_{kjl}}{P^{\mathrm{suc,ref}}_{kjl}}\right)^{(k^{\mathrm{isen}}-1)/k^{\mathrm{isen}}} - 1}\right] \tag{57}$$

4.2.2. Constraints general to all plants

Eq. (12), Eq. (13) and Eq. (15) are the same as for the planning model, while Eq. (14) and Eq. (16) are adjusted in Eq. (58) and Eq. (59) to reflect the fixed binary variables. Eq. (58) and Eq. (59) are valid for all $j \in J$ and $t \in T$. The calculation of total flow from Eq. (17) is redundant, since this is only required for the price calculations and prices are fixed for the scheduling model. In addition, the logic from Eq. (18) and Eq. (19) is redundant and excluded.

$$L_j^{\mathrm{H_2\_flow}}\overline{y_{jt}}\ \mathrm{H_2} \le \mathrm{flow}_{jt} \le U_j^{\mathrm{H_2\_flow}}\overline{y_{jt}} \tag{58}$$

$$\mathrm{auxpower}_{jt} = \mathrm{aux}^1_j\overline{y_{jt}} + \mathrm{aux}^2_j(\mathrm{H_2flow}_{jt} - \mathrm{aux}^3_j\overline{y_{jt}}) \tag{59}$$

4.2.3. Constraints specific to offgas plants

Eq. (20) through Eq. (25) from the planning model are exactly duplicated on the scheduling level. The offgas price is fixed from the planning level and only the hydrogen production from the current period is used to calculate the feed cost, yielding Eq. (60), which is valid for all $j \in \mathrm{OG}$, and $t \in T$. Eq. (27) and Eq. (29) and disjunction Eq. (28a) and Eq. (28b) are thus redundant. The duration of the time period is now 1 h.

$$\mathrm{feedcost}_j = \overline{\mathrm{ogprice}_j}\sum_t (\mathrm{H_2flow}_{jt}\mathrm{duration}_t)\mathrm{H_2purity}_j \tag{60}$$

4.2.4. Constraints specific to 'on-demand' plants

Eq. (30) is adjusted to incorporate the fixed binary to yield Eq. (61) and the natural gas price is fixed from the planning problem and used together with the natural gas flow for the current period to calculate the feed cost in Eq. (62). Eq. (31) and Eq. (34) and disjunction Eq. (33a) are thus not present in the scheduling model. The steam flow calculation is adjusted to incorporate the fixed binary in Eq. (63) and Eq. (64), and the fixed steam credit in Eq. (65), while Eq. (36) remains the same and Eq. (39) is not required. Eq. (61) through Eq. (65) are valid for all $j \in \mathrm{OD}(J)$ and $t \in T$.

$$\mathrm{ngflow}_{jt} = a_{0j}\overline{y_{jt}} + a_{1j}\mathrm{H_2flow}_{jt} + a_{2j}\mathrm{H_2flow}^2_{jt} + a_{3j}\mathrm{H_2flow}^3_{jt} \tag{61}$$

$$\mathrm{feedcost}_j = \overline{\mathrm{ngprice}_j}\sum_t(\mathrm{ngflow}_{jt}\mathrm{duration}_t) \tag{62}$$

$$\mathrm{steamflow}_{jt} = (a_{0j}\overline{y_{jt}} + a_{1j}\mathrm{H_2flow}_{jt} + a_{2j}\mathrm{H_2flow}^2_{jt})/c_j^{\mathrm{steam}} \tag{63}$$

$$\mathrm{steamexp}_{jt} \le U_j^{st,\exp}\overline{y_{jt}} \tag{64}$$

$$\mathrm{steamrev}_{jt} = \overline{\mathrm{steamcred}_j}\mathrm{steamexp}_{jt}\mathrm{duration}_t \tag{65}$$

4.2.5. Energy cost calculations general to all plants

The primary and secondary kWh values, as well as the average power consumption, are fixed from the planning model. The power cost is then calculated as shown in Eq. (66), which is valid for all $j \in J$ and $t \in T$. Only the power from the current period is used in the calculation, and the duration of the time period has been set to 1 h. Eq. (42) through Eq. (51) are not present in the scheduling model.

$$\mathrm{powercost}_j = c_j^{\mathrm{base}}\sum_t \mathrm{plantpower}_{jt}\mathrm{duration}_t + \left[\frac{(c_j^{\mathrm{prim}}\overline{\mathrm{primKWHR}_j} + c_j^{\mathrm{scnd}}\overline{\mathrm{scndKWHR}_j})}{\overline{\mathrm{avgpower}_j}24\ \mathrm{days}}\right] \times \sum_t \mathrm{plantpower}_{jt}\mathrm{duration}_t \tag{66}$$

4.3. Pipeline model

The pipeline constraints for the scheduling model are more complex than for the planning model in that they include descriptions of the pressure gradients required to satisfy demands at contract pressures. We use the same network of nodes and arcs as for the planning model, but pressure levels are now allowed to vary within each pipeline and for each compressor discharge point. All pipeline constraints are valid for all $(n,n') \in \mathrm{arc}(n,n')$ and $t = T$, except where otherwise indicated. The mass balances over each node (Eq. (52)) and the plant flow and customer flow calculations (Eq. (53) and Eq. (54))

remain the same as for the planning model. For the inventory calculation, the average pressure between the node, and the midpoint of each arc connected to it, is used instead of a constant average pipeline pressure as shown in Eq. (67).

$$\mathrm{inv}_{n,t} = \frac{\pi}{8}\Bigg[\sum_{\substack{n' \in [\mathrm{arc}(n,n') \\ \cap n\_\mathrm{pipe}(h2l,n')]}} \frac{D^2_{n,n'} L_{n,n'}(P^{\mathrm{node}}_{n,t} + P^{\mathrm{arc}}_{n,n',t})}{2R_{\mathrm{g}}T_{\mathrm{abs}}} + \sum_{\substack{n' \in [\mathrm{arc}(n',n) \\ \cap n\_\mathrm{pipe}(h2l,n')]}} \frac{D^2_{n,n'} L_{n',n}(P^{\mathrm{node}}_{n,t} + P^{\mathrm{arc}}_{n',n,t})}{2R_{\mathrm{g}}T_{\mathrm{abs}}}\Bigg] + s1^{\mathrm{inv}}_{n,t} - s2^{\mathrm{inv}}_{n,t} \tag{67}$$

$\forall (n, h2l) \in n\_\mathrm{pipe}(h2l, n),\quad t \in T$

The arc pressure is the average of the pressures at the nodes at its endpoints:

$$P^{\mathrm{arc}}_{n,n',t} = \frac{P^{\mathrm{node}}_{n,t} + P^{\mathrm{node}}_{n',t}}{2} \tag{68}$$

The pressure for the applicable node is set equal to the discharge pressure from the compressor connected to it:

$$p^{\mathrm{dis}}_{k,j,h2l,t} = P^{\mathrm{node}}_{n,t}$$
$$\forall (k,j,h2l) \in k^{\mathrm{config}}(k,j,h2l), (n,j) \in p\_\mathrm{node}(j,n),\quad t \in T \tag{69}$$

Eq. (70) models the pressure drop in the pressure control valves between pipelines at different pressure levels.

$$\Delta P^{\mathrm{valve}}_{n,n',t} = P^{\mathrm{node}}_{n,t} - P^{\mathrm{node}}_{n',t}$$
$$\forall ((n,n') \in \mathrm{arc}(n,n')) \cap ((n,h2l) \in n\_\mathrm{pipe}(h2l,n)) \cap ((n',h2l') \in n\_\mathrm{pipe}(h2l',n')),\quad t \in T \tag{70}$$

To model the pressure gradients through the pipeline, the Reynolds number is first calculated as follows

$$\mathrm{Re}_{n,n',t} = \frac{4|\mathrm{flowarc}_{n,n',t}|M}{\pi D_{n,n'}\mu} \tag{71}$$

This calculation requires the absolute value, indicated by $|\mathrm{flowarc}_{n,n',t}|$, of the flow in the arc, since the flow can be positive or negative depending on the direction of flow. A smooth approximation is used to model this absolute value, since it is a discontinuous function that causes problems for nonlinear programming solvers, and Eq. (71) thus becomes Eq. (72) and Eq. (73) with δ a small number, in this work found to be most effective at a value of 0.0001.

$$\mathrm{Re}_{n,n',t} = \frac{4\mathrm{absflow}_{n,n',t}M}{\pi D_{n,n'}\mu} \tag{72}$$

$$\mathrm{absflow}_{n,n',t} = \sqrt{\mathrm{flowarc}^2_{n,n',t} + \delta^2} \tag{73}$$

We need to mention that other formulations were tried for the absolute value, such as a smooth approximation from Bullard (1991) a disjunctive formulation with integer variables (and relaxed integers) where the flow is expressed as the difference between two positive numbers, and using the abs function from GAMS directly with the DNLP method (see Brooke, Kendrick & Meeraus, 1992). However, we found that the smooth approximation given here is the only one that yields reasonable feasible solutions.

The friction factor is a function of the Reynolds number. If the flow is laminar, the following correlation holds

$$f_{n,n',t} = \frac{64}{\mathrm{Re}_{n,n',t}} \tag{74}$$

while if the flow is turbulent, the correlation given in Eq. (75) is used.

$$f_{n,n',t} = \frac{a^{\mathrm{turb}}_{n,n'}}{\left[\log\left(b^{\mathrm{turb}}_{n,n'}\frac{\varepsilon_{n,n'}}{D_{n,n'}} + \frac{c^{\mathrm{turb}}_{n,n'}}{\mathrm{Re}_{n,n',t}}\right)\right]^2} \tag{75}$$

The nonlinearities present in Eq. (75) also cause problems for nonlinear solvers, and we therefore replace it with an approximation in the form of a log-linear line. This line is easily obtained by calculating two points from Eq. (75), taking their logarithms and joining them with a log-linear line to yield Eq. (76), where m and c are the slope and intercept of the line, respectively.

$$\log(f_{n,n',t}) = m_{n,n'}\ \log(\mathrm{Re}_{n,n',t}) + c_{n,n'} \tag{76}$$

When plotted on a log scale, it turns out that the valid correlation is always the one that yields the larger friction factor, and it is thus sufficient to replace Eq. (74) and Eq. (76) with Eq. (77):

$$\log(f_{n,n',t}) = \max[\log(64) - \log(\mathrm{Re}_{n,n',t});\ m_{n,n'}\ \log(\mathrm{Re}_{n,n',t}) + c_{n,n'}] \tag{77}$$

This max function again needs to be reformulated to avoid discontinuities. For the max functions earlier in the paper, we used discrete variables to determine which function is valid. However, for the pipeline model, we want to avoid having a binary variable for each arc, since this will cause intractability and increased problems with infeasible solutions. We therefore use a formulation from Sahinidis and Grossmann (1992) as shown in Eqs. (78)–(81) with the λ's being binary variables that are relaxed to take any value between 0 and 1. We found that this formulation nearly consistently resulted in 0 or 1 values for the relaxed binaries.

$$\log(f_{n,n',t}) \geq \log(64) - \log(\mathrm{Re}_{n,n',t}) \tag{78}$$

$$\log(f_{n,n',t}) \geq m_{n,n'}\log(\mathrm{Re}_{n,n',t}) + c_{n,n'} \tag{79}$$

$$\log(f_{n,n',t}) \leq \lambda^1_{n,n',t}(\log(64) - \log(\mathrm{Re}_{n,n',t})) + \lambda^2_{n,n',t}(m_{n,n'}\ \log(\mathrm{Re}_{n,n',t}) + c_{n,n'}) \tag{80}$$

$$\lambda^1_{n,n',t} + \lambda^2_{n,n',t} = 1 \tag{81}$$

The pressure gradient across each arc from n to n' is approximated by the difference between the end pressure at in′ and the beginning pressure at n, divided by the arc length:

$$dpdz_{n,n',t} = \frac{P^{\text{node}}_{n',t} - P^{\text{node}}_{n,t}}{L_{n,n'}} \tag{82}$$

In addition, the pressure gradient is expressed by Eq. (83), where $\text{sgn}(\text{flowarc}_{n,n',t})$ indicates the sign (+ or −) or direction of flow.

$$dPdz_{n,n',t} = -\text{sgn}(\text{flowarc}_{n,n',t}) \times \frac{8f_{n,n',t}\text{flowarc}^2_{n,n',t}}{\pi^2 D^5_{n,n'} P^{\text{arc}}_{n,n',t}} R_g T_{\text{abs}} c^{dPdz} M \tag{83}$$

Once again the problems caused for nonlinear solvers by the 'sign' expression, can be overcome by reformulating the general expression $\text{sign}(x)x^2 = |x|x$, where $|x|$ indicates the absolute value of x, with which Eq. (84) becomes:

$$dPdz_{n,n',t} = -\text{absflow}_{n,n',t}\text{flowarc}_{n,n',t} \times \frac{8f_{n,n',t}}{\pi^2 D^5_{n,n'} P^{\text{arc}}_{n,n',t}} R_g T_{\text{abs}} c^{dPdz} M \tag{84}$$

4.3.1. Optional integration constraints

To facilitate better integration between the planning level and scheduling level, targets for power consumption and hydrogen flow can be set for the scheduling level with the results from the planning level. If these targets can be satisfied within a reasonable tolerance, the feed and energy prices that are fixed on the scheduling level would be acceptable if the targets are not satisfied the actual prices might end up being different than predicted from the planning level, but the outcome can only be established after the complete planning horizon. Eq. (85) and Eq. (86) state that the power and hydrogen production in each scheduling period should equal the targets from the planning level with two positive slacks that allow deviations from the targets. These constraints are valid for all $j \in J$ and $t \in T$. The slacks are minimized in the objective function.

$$\text{plantpower}_{jt} = \overline{\text{plantpower}^{\text{plan}}_{jt}} + s1^{\text{linkpower}}_{j,t} - s2^{\text{linkpower}}_{j,t} \tag{85}$$

$$\text{H}_2\text{flow}_{jt} = \overline{\text{H}_2\text{flow}^{\text{plan}}_{jt}} + s1^{\text{linkflow}}_{j,t} - s2^{\text{linkflow}}_{j,t} \tag{86}$$

We found that the addition of Eq. (86) to the current model has the result that the hydrogen flow meets the target exactly. However, the addition of Eq. (85) to the current model results in infeasible solutions. This is due to the nonlinear nature of the scheduling model, and it is clear that these nonlinearities need to be addressed further to allow better integration and implementation in practice. For the purpose of this work, we thus include only Eq. (86), while Eq. (85) is mentioned in consideration of future work.

4.3.2. Objective

The objective of the scheduling level is to minimize costs for the single period (see Eq. (87)) and includes power costs, feed costs and steam revenues for all the plants, as well as the slacks from Eq. (67), Eq. (85) and Eq. (86) multiplied by an appropriate weight.

$$\begin{aligned}\min Z = &\sum_j \left(\text{powercost}_j + \text{feedcost}_j - \sum_{t=1} \text{steamrev}_{jt}\right) \\ &+ \sum_n \sum_t w^{\text{inv}}(s1^{\text{inv}}_{n,t} + s2^{\text{inv}}_{n,t}) \\ &+ \sum_j \sum_t w^{\text{linkpower}}(s1^{\text{linkpower}}_{j,t} + s2^{\text{linkpower}}_{j,t}) \\ &+ \sum_j \sum_{t=1} w^{\text{linkflow}}(s1^{\text{linkflow}}_{j,t} + s2^{\text{linkflow}}_{j,t})\end{aligned} \tag{87}$$

In addition, lower and upper bounds are specified for all variables, but not shown here.

5. Example 1

To illustrate the proposed method, we solve a small example consisting of all plants and pipelines, but only eight time periods (4 days). In this example, the number of peaks used in the energy price calculations, N^{peak}, equals 2 for both the on- and off-peak calculations. First the planning level is solved to set the prices and production targets. Fig. 7 shows the total hydrogen production for each planning period versus the total demand normalized to a peak of 100 and it can be seen that the production closely follows the demand. There are, however, periods of over- or underproduction of 1–

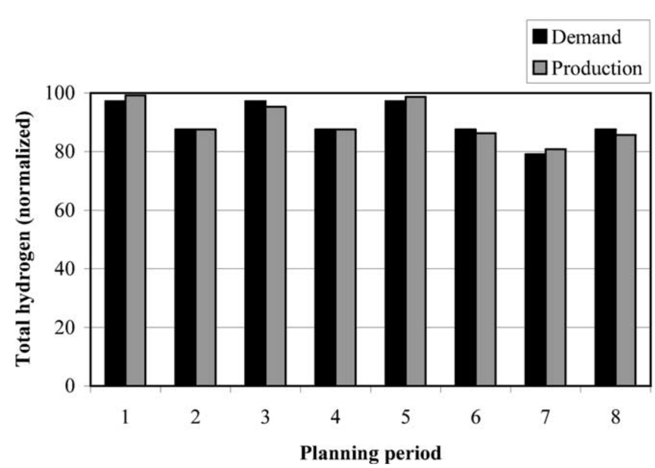

Fig. 7. Demand versus production for Example 1.

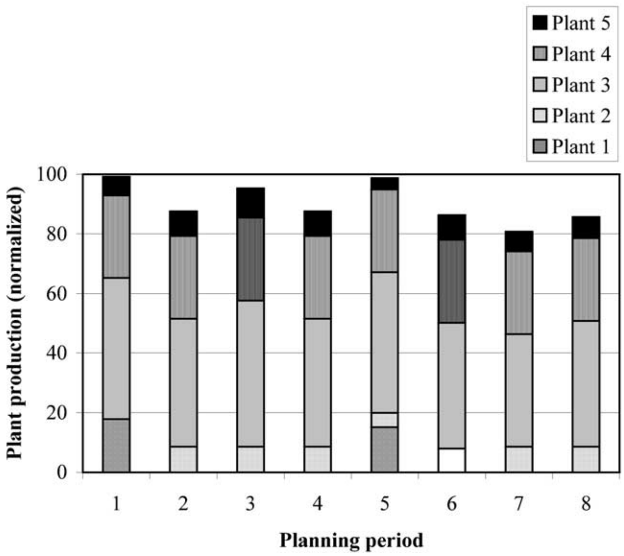

Fig. 8. Hydrogen production from each plant for Example 1.

2%. Note that the values in the graph below are normalized to 100 and that 1 or 2% of the total production from five gas plant is a significant number. In this case, significant enough to allow production levels that deviate from actual demand by using the pipeline as inventory, thereby leading to production in a lower price increment. This is explained further in the next two paragraphs with a specific example.

Note that the demand is exactly satisfied even when the production is not equal to the demand, since the difference is accounted for through the pipeline inventory. This feature demonstrates how the pipeline can be used for inventory purposes to allow manipulation of the feed and energy prices. To expand on this idea, consider also Fig. 8, which shows the hydrogen production from each plant as a part of the total production.

It can be seen, for example, that plant 1 produces only close to its maximum amount in offpeak periods 1 and 5, and nothing for the rest of the planning horizon. By doing so, the total production is higher than the demand for those periods as seen in Fig. 7, thereby increasing the inventory and one may ask why more is produced than there is a demand for. It turns out that in the energy price calculation, this production level has the effect that the third disjunctive term of disjunction (Eq. (49a)) becomes valid, with the result that a low primKVA value is used. This value leads to a low primKWHR value and finally a low total energy price for plant 1. Non-obvious trade-offs such as this one would not be captured if the complex pricing rules were not included explicitly in the optimization model.

After the planning problem has been solved, the energy and feed prices are fixed and the reactive scheduling model is solved sequentially for 12 h-long time periods, i.e for the first planning period. For illustration purposes, we assume that the actual demands are equal to the predicted demands. Due to the presence of Eq. (86), the hydrogen production target for each plant is exactly satisfied in each scheduling period. Fig. 9 shows the normalized power consumption for each plant according to the planning model, compared to the outcome from the reactive scheduling level for the first planning period. It can be seen that the power consumption is very close and this indicates that there is a good correlation between the two levels.

In reality the actual demands may differ significantly from the predicted demand and the success of integration depends on how large these differences are. We solve the eight period model for the cases where the actual demands are 10% higher and 10% lower than the predicted demands. Again, the hydrogen production from each plant meets the target exactly, while Fig. 10 shows the average power consumption for each plant compared to the planned consumption. It can be seen that in general less power is required when the demand is more than predicted, while more power is required when the demand is less than predicted, if the hydrogen production remains the same. This follows from the realization that when the demand increases while the production remains the same, the inventory and pipeline

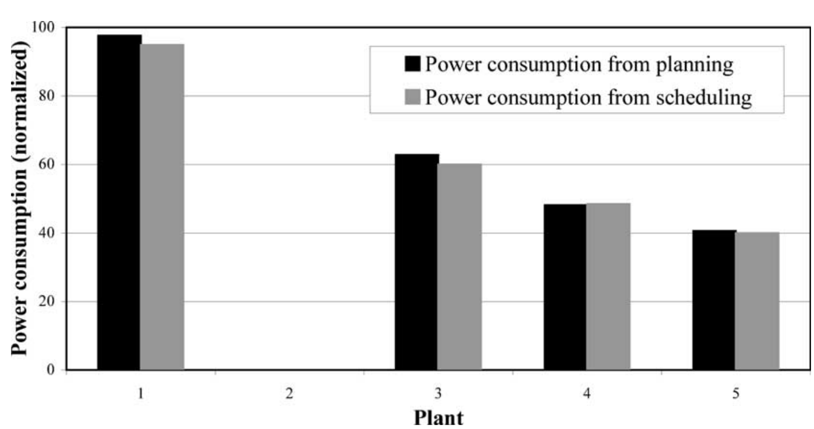

Fig. 9. Planned power consumption versus outcome from scheduling level for first planning period.

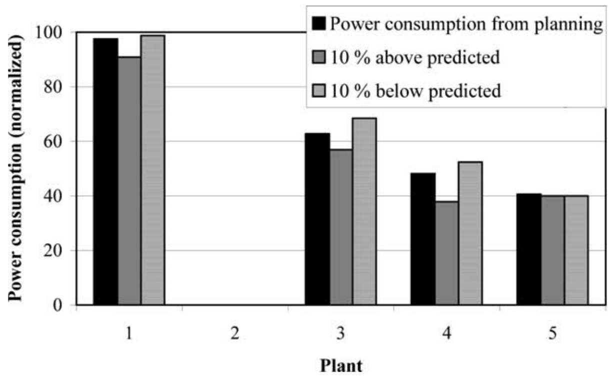

Fig. 10. Power consumption for deviations in actual demand from predicted, for first planning period.

pressure decrease. Since the compressor discharge pressure is linked to the pipeline pressure, this also decreases and the result is less power for the same flow according to Eq. (1). The opposite argument can be made for a decrease in demand. If the hydrogen production should be allowed to change to investigate the effects of demand changes, the weights for the associated slack variables can be decreased. However, this will not guarantee a better power correlation, unless Eq. (85) is added to the model.

To see if it is necessary to model the pipeline in detail on the scheduling level, we look at the pressure values and see if these are realistic and significantly different from their average value. Fig. 11(a)–(d) show the normalized pressures at a subset of consecutive nodes for each pressure level from the first reactive scheduling period. These graphs indicate realistic pressure profiles showing pressures that vary between different ranges for the different pipelines, from the P_4 pipeline where there is no variation, to the P_3 pipeline where the pressure difference between two endpoints varies significantly. These varying pressures indicate that including variable

Table 1
Problem sizes and solution times for Example 1

	Planning model	Reactive scheduling model
Constraints	4897	1466
Continuous variables	6322	1703
Discrete variables	255	124
Solution time (CPI s^{-1})	136.1	9.4

pressures along the pipeline instead of using an average pressure is important for accurate reactive scheduling of pipeline systems, since the pressure at a specific point can differ significantly from the average pressure. Knowing the actual pressures are important, since these values determine the pressure gradient, which in turn determines the flow rates, etc.

Table 1 shows the problem sizes and the solution times for the multiperiod planning and single period scheduling models. The models are written in GAMS (Brooke et al., 1992) and solved with the MINLP solver DICOPT++ (Viswanathan and Grossmann, 1990) on a Pentium III 667 MHz machine. The MILP master problems are solved with CPLEX 7.0 (ILOG, 2001), while the NLP subproblems are solved with CONOPT2 (Drud, 1994). For the planning time reported in Table 1, one iteration of DICOPT++ was used and the scheduling time reflects the average of the 12 subproblems.

As can be seen, even for this small instance the planning level requires more than ten times the computational effort of the average scheduling model. The scheduling model does not scale with time, since single period models are run in sequence on this level. The planning model, however, does scale with additional time periods and very quickly becomes intractable. For example, when the number of time periods in this example is increased to 14 to constitute 1 week of

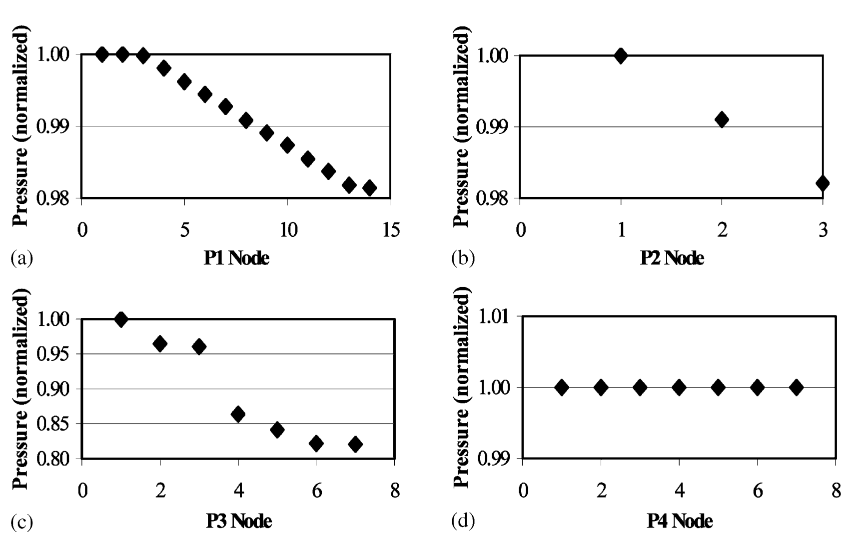

Fig. 11. (a–d): Pressure variation along different pipeline levels.

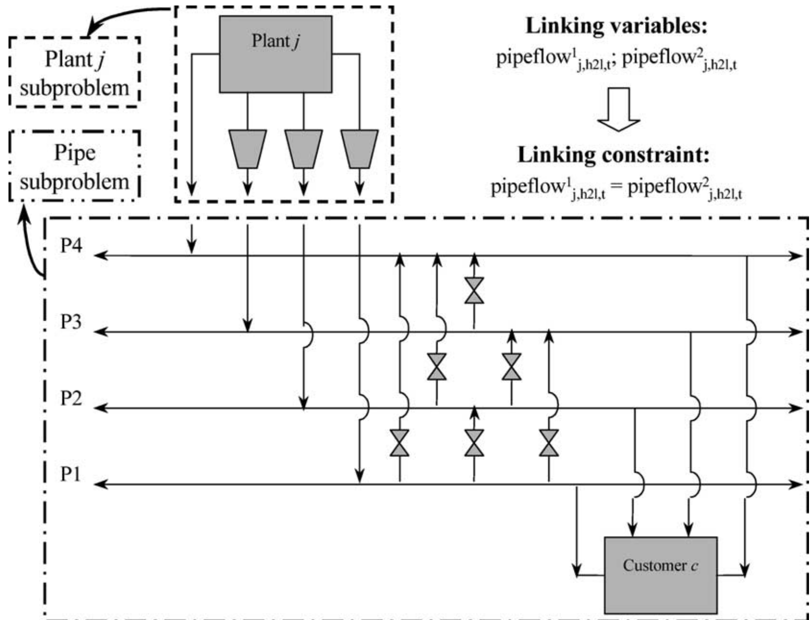

Fig. 12. Lagrangean decomposition subproblems, with linking variables and constraint.

planning, the size of the model nearly doubles to 8353 constraints, 10942 continuous variables and 405 discrete variables. For this instance, no solution for even the first MILP could be obtained in more than 40,000 CPU s when using DICOPT++. This indicates the need for a specialized solution algorithm for the planning level.

6. Solution approach for the planning level

We propose a heuristic based on ideas from Lagrangean decomposition, where the original model is decomposed into six Lagrangean subproblems, namely one for each plant and one for the pipeline. The choice of subproblems is motivated by the fact that each plant has its own complex pricing structure and the only link between the plants and the pipeline on the planning level is the hydrogen flow.

Lagrangean decomposition was first proposed by Guignard and Kim (1987). The basic idea is to identify in a model blocks of constraints that are linked by only a few variables. Copies of these ‘linking’ variables are made and one copy is assigned to each constraint block where the original variable appears. Equality constraints are added to set the copies equal to the original variable and the ‘linking’ variables have now been replaced by ‘linking’ constraints. These constraints can be removed according to Lagrangean relaxation to yield a decomposable model. The removed constraints are replaced by a penalty term in the objective function, consisting of the deviation in the removed constraint multiplied by the associated Lagrange multiplier.

The planning model presented in Section 4.1 is ideally suited for Lagrangean decomposition, since the pipeline and each plant has its own model, and the only linking is due to the flow between the plants and the pipelines ($\text{pipeflow}_{j,h2l,t}$). In our approach, these variables are duplicated with superscript 1 for the plant subproblems, and superscript 2 for the pipe subproblem. They are then set equal in linking constraints, and these equality constraints consequently relaxed to yield a decomposable model (see Fig. 12). The lower bounding properties associated with the Lagrangean dual cannot be used here, due to the presence of non-convexities. We therefore use a heuristic approach where the Lagrangean decomposition is used to quickly generate good integer points, while an upper bounding NLP is solved to generate true feasible solutions (see also Van den Heever, Grossmann, Edwards & Vasantharajan, 2001).

Fig. 13 shows the heuristic as applied in this work. The Lagrange multipliers are initialized by solving the relaxed model. Subsequently, the pipeline and plant subproblems are solved to help generate a feasible solution. First, the pipeline subproblem is solved to determine which pipelines should expect flows from which plants and then each plant is optimized with the condition that it has to supply at least half of the flow required from the pipeline subproblem. This heuristic rule is used to help eliminate infeasible solutions to the simultaneous problem in the next step, where the integer variables from the plant subproblems are fixed and an NLP is solved for the pipeline and plants simultaneously. The solution to the NLP is an upper bound to the original problem and represents a feasible solution if the slack variables in Eq. (55) equal zero. Note that although the sum of the objectives from the subproblems is not guaranteed to give a lower bound, they still yield an estimate to the solution of the

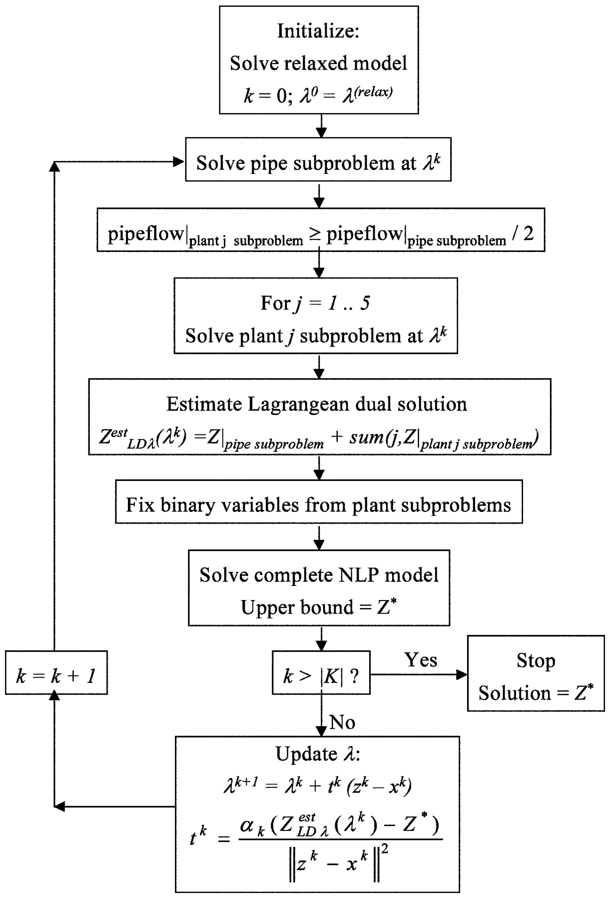

Fig. 13. Lagrangean decomposition heuristic.

Lagrangean dual. This estimate is then used, together with the upper bound and the deviation in the linking constraints, to update the Lagrange multipliers according to a subgradient updating procedure. This is a well-known updating scheme (see Fisher, 1985), where α_k is a scalar, t^k is a scalar stepsize and z^k, x^k are optimal values of the duplicate variables from the Lagrangean subproblems with the multipliers set to λ^k. Since there are no guarantees for convergence or optimality associated with this method, it is terminated after a pre-specified iteration limit, or after no improvement in the upper bound in a number of iterations. For the purpose of this work, the termination criterion is ten iterations.

In our implementation, all NLPs are solved with CONOPT2 (Drud, 1994), while all MILPs are solved with CPLEX 7.0 (ILOG, 2001). All MINLP subproblems are solved with one DICOPT++ iteration, with the same MILP and NLP solvers as indicated before. The models are formulated with GAMS (Brooke et al., 1992) and run on a Pentium III 667 MHz machine. In previous work (Van den Heever et al., 2001), we presented a similar heuristic approach for the planning of offshore hydrocarbon infrastructures with complex economic rules. We therefore do not go into more theoretical background detail here. However, we refer the interested reader to the work of Fisher (1981, 1985), in which he describes heuristic approaches for the solution of the Lagrangean dual and the implementation of these heuristics.

Table 2
Computational comparison between DICOPT++ and proposed method

	DICOPT++	Proposed method
Eight periods		
Cost (normalized)	30.3	30.1
Solution time (CPU s)	136.1	358.1
14 periods		
Cost (normalized)	–	50.9
Solution time (CPU s)	> 40,000	1367.4

7. Example 1 revisited

We apply the proposed Lagrangean decomposition heuristic to both the eight period and 14 period planning instances from Example 1 to compare the performance of the proposed heuristic with DICOPT++. Table 2 shows the respective solution times and objective values for both methods. The objective values have been normalized to a value out of 100 for confidentiality reasons, where 100 represents the cost for a 2 week horizon (see Example 2).

It can be seen that the proposed method finds an objective value slightly better than that obtained from DICOPT++, but requires more CPU time for the eight period problem. However, the computational benefit of the proposed method is demonstrated for the 14 period problem where DICOPT++ could not find a solution in more than 40,000 CPU s, while the proposed method finds an objective of 50.9 in only 1367.4 CPU s. This is clearly more than an order of magnitude reduction in solution time. While the reported time is for ten iterations, the best solution was found in the fourth iteration. The reduction in solution time arises from the fact that the combinatorics associated with the discrete variables are significantly reduced when the plants are solved separately, as seen in Table 3. This table shows the typical problem sizes and solution times for the subproblems in the proposed Lagrangean decomposition heuristic taken from the best solution. It is clear that the most computationally intensive part of the problem has now moved from the MILP part to the NLP upper bounding problem.

Table 3
Problem sizes and solution times for subproblems from the 14 period problem

Subproblem	Constraints	Continuous variables	Discrete variables	Solution time (CPU s)
Pipeline	4831	7351	0	0.9
Plant 1	587	604	81	1.5
Plant 2	704	829	83	1.2
Plant 3	770	654	85	1.2
Plant 4	865	1087	81	1.3
Plant 5	671	618	81	0.8
Upper bounding NLP	8465	11459	0	93.5

Table 4
Problem sizes and solution times for subproblems for 28 period problem

Subproblem	Constraints	Continuous variables	Discrete variables	Solution time (CPU s)
Pipeline	9661	14701	0	2.0
Plant 1	1207	1180	207	9.7
Plant 2	1436	1629	209	8.2
Plant 3	1558	1272	211	6.6
Plant 4	1765	2105	207	10.7
Plant 5	1375	1208	207	3.7
Upper bounding NLP	17081	22991	0	578.2

8. Example 2

For the proposed methodology, the planning model needs to be solved for 2 weeks, or 28 periods and this should be accomplished in less than 12 h to be in time for the reactive scheduling. In addition, three peaks instead of two need to be used for the energy price calculations, leading to an additional increase in problem size. As was demonstrated in the previous paragraph, solving the 28 period problem in the full space with DICOPT++ is not possible and when attempting this, no feasible solution could be found in several days. We therefore apply the proposed Lagrangean decomposition heuristic to the 28 period problem, with the result of obtaining an objective cost of 100 in less than 1.5 h (4220 CPU s) for ten iterations. In this case, the best solution was found in the third iteration. Table 4 shows the problem sizes and solution times for each subproblem corresponding to the best solution.

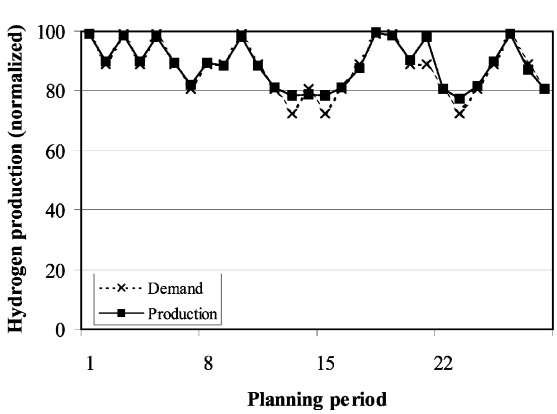

Fig. 14. Total production versus demand for 2 week horizon.

Fig. 14 shows the normalized total production for each time period compared to the predicted demand and it can be seen that the overall production is in general greater than the demand, with in some cases differences greater than 10%. Note that the graph is normalized and a difference of 10% represents a substantial magnitude difference considering that the number equals the total production from five hydrogen plants. This once again illustrates how the pipeline is used as inventory allowing production greater than the actual demand to achieve a lower cost increment.

Fig. 15 shows the hydrogen contribution from each plant in each time period for the 2 week planning horizon.

When comparing the first planning period from the 2 week horizon with the first 12 h of reactive scheduling, the hydrogen production target is met exactly. Fig. 16 shows the normalized power consumption for each plant from the first planning period compared to the average of the first 12 scheduling periods. It can be seen that the average power consumption from the scheduling periods is very close to that from the planning model. However, deviations exist possibly due to the relaxation of the load step binaries on the planning level, and to the fact that the scheduling level is solved as sequential single period models instead of a multiperiod model.

Finally, we need to point out that the proposed planning problem yields significant improvements over the planning model used in the past for this hydrogen supply network. In the past a lumped demand, without

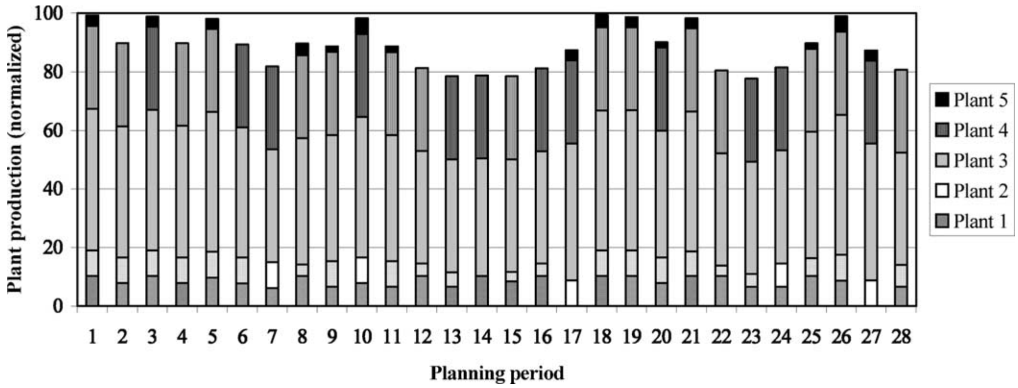

Fig. 15. Hydrogen contribution from each plant for 2 week planning horizon.

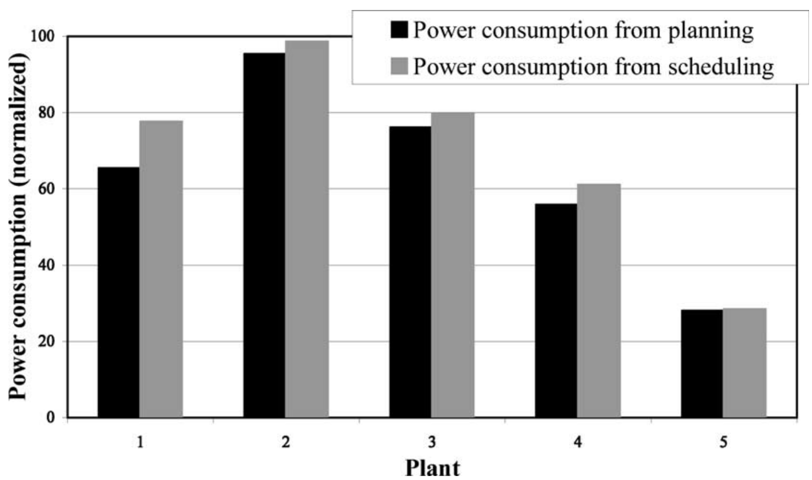

Fig. 16. Power consumption for first planning period.

considering the pressure requirements or pipeline network, were used for planning purposes. In addition, a fixed price for energy was assumed. In contrast, not only does the proposed model include specific customer demands at specified pressure levels as well as the pipeline network, but production and inventory can also be manipulated to obtain lower energy prices and thus lowered costs. The magnitude or percentage of expected savings due to this inclusion cannot be stated here for reasons of confidentiality, but it is significant. The proposed model yields a more accurate solution of plant production and power consumption in order to satisfy customer demands at contract pressures, while minimizing costs. On the scheduling level, significant improvements were also made for this specific network. In the past, scheduling was carried out according to the results from the planning level, without considering pipeline dynamics or compressor loadstep constraints. In the proposed model, detailed pipeline dynamics, plant models, compressor load step constraints and a detailed network are included for accurate and feasible reactive scheduling.

9. Conclusions

A methodology for the integrated production planning and reactive scheduling in the optimization of a hydrogen supply network was proposed. This method relies on a two-level decomposition where the upper level involves a multiperiod MINLP planning model and the lower level involves a multi/single period MINLP reactive scheduling model. The planning model determines feed and energy prices, as well as production targets and includes detailed economic calculations for each plant, with a simplified pipeline model. The scheduling model determines the compressor operation as actual demands become known, with fixed prices and production targets from the planning model and a detailed pipeline model. A Lagrangean decomposition heuristic is presented to address the computational effort involved in solving the planning model, while the reactive scheduling model is solved as sequential single period models. Information is passed between the planning and scheduling models as they are solved in a rolling horizon fashion each 12 or 1 h, respectively.

Results show that the proposed Lagrangean decomposition heuristic shows more than an order of magnitude reduction in solution time compared to a full space approach using DICOPT++, while obtaining solutions of similar or better quality. In addition, the production levels from the scheduling level correspond exactly to those of the planning level, while the power consumption from the scheduling level is close to that of the planning level. Some discrepancies exist that we believe are due to (1) nonlinearities on the scheduling level; (2) relaxation of the load step variables on the planning level; and/or (3) solving the scheduling sequentially instead of simultaneously. These issues are the subject of future work.

The proposed methodology has shown to successfully integrate the production planning and reactive scheduling levels, apart from the before mentioned discrepancies. In addition, the planning level addresses pricing issues that have never been considered before in the literature to yield significantly lower costs. Also, the scheduling level involves the most inclusive reactive scheduling model for gas pipeline distribution networks to date, in that the model incorporates plant models, compressor models, detailed pipeline dynamics, inventory calculations and the detailed large-scale pipeline network.

Acknowledgements

The authors would like to acknowledge financial support from Air Products and from the Department of Energy under Grant No. DE-FG02-98ER14875. The authors would also like to thank Professor Larry Biegler for useful discussions.

References

Balas, E. (1985). Disjunctive programming and a hierarchy of relaxations for discrete optimization problems. *SIAM J. Alg. Disc. Meth. 6*, 466–486.

Bassett, M. H., Dave, P., Doyle, F. J., III, Kudva, G. K., Pekny, J. F., Reklaitis, G. V., Subramanyam, S., Miller, D. L., & Zentner, M. G. (1996). Perspectives on model based integration of process operations. *Comput. Chem. Engng. 20*, 821–844.

Birewar, D. B., & Grossmann, I. E. (1990). Simultaneous production planning and scheduling of multiproduct batch plants. *Ind. Eng. Chem. Res. 29*, 570.

Bose, S., & Pekny, J. F. (2000). A model predictive framework for planning and scheduling problems: a case study of consumer goods supply chain. *Comput. Chem. Eng. 24*, 329–335.

Brooke, A., Kendrick, D., & Meeraus, A. (1992). *GAMS: A User's Guide, Release 2.25*. South San Francisco: The Scientific Press.

Bullard, L.G., Iterated linear programming strategies for constrained and nonsmooth simulation, Ph.D. Dissertation, Carnegie Mellon University, 1991.

Bullard, L. G., & Biegler, L. T. (1992). Iterated linear programming strategies for nonsmooth simulation: continuous and mixed-integer approaches. *Comput. Chem. Eng. 16* (1992), 949–961.

Coxhead, R. E. (1994). Integrated planning and scheduling systems for the refining industry. In T. A. Ciriani & R. C. Leachman (Eds.), *Optimization in Industry 2* (pp. 185–199). New York: Wiley and Sons.

Das, B. P., Rickard, J. G., Shah, N., & Macchietto, S. (2000). An investigation on integration of aggregate production planning, master production scheduling and short-term production scheduling of batch process operations through a common data model. *Comput. Chem. Eng. 24*, 1625–1631.

Dimitriadis, A. D., Shah, N., & Pantelides, C. C. (1997). RTN-based rolling horizon algorithms for medium term scheduling of multipurpose plants. *Comput. Chem. Eng. S21*, S1061.

Drud, A. (1994). CONOPT—a large scale GRG code. *ORSA J. Comput. 6*, 207.

Duran, M., & Grossmann, I. E. (1986). A mixed-integer nonlinear programming algorithm for process systems synthesis. *AIChE J. 32* (4).

Fisher, M. L. (1981). The Lagrangean relaxation method for solving integer programming problems. *Manage. Sci. 27* (1).

Fisher, M. L. (1985). An applications oriented guide to Lagrangean relaxation. *Interfaces 15* (2), 10.

Guignard, M., & Kim, S. (1987). Lagrangean decomposition: a model yielding stronger Lagrangean bounds. *Math. Prog. 39*, 215.

Grossmann, I.E., Van den Heever, S.A., Harjunkoski, I., 'Discrete Optimization Methods and their Role in the Integration of Planning and Scheduling,' AIChE Symposium Series No 326, Vol. 98 pp. 150–168 (2002).

ILOG CPLEX 7.0, User's Manual, ILOG Inc., 2001.

Lasschuit, W., Thijssen, N., Supporting Supply Chain Planning And Scheduling Decisions in the Oil and Chemical Industry, Proceedings FOCAPO 2003 (Eds. I.E. Grossmann and C.M. McDonald), pp. 37–44, CACHE.

Marques, D., & Morari, M. (1988). On-line optimization of gas pipeline networks. *Automatica 24* (4), 455–469.

Martinez-Benet, J. M., & Puigjaner, L. (1988). A powerful improvement on the methodology for solving large-scale pipeline networks. *Comput. Chem. Eng. 12* (2/3), 261–265.

Neiro, S.M.S., Pinto, J.M. Supply Chain Optimization of Petroleum Refinery Complexes, Proceedings FOCAPO 2003 (Eds. I.E. Grossmann and C.M. McDonald), pp. 59–72, CACHE.

Papageorgiou, L. G., & Pantelides, C. C. (1996a). Optimal campaign planning/scheduling of multipurpose batch/semi-continuous plants, 1. Mathematical formulations. *Ind. Eng. Chem. Res. 35*, 488.

Papageorgiou, L. G., & Pantelides, C. C. (1996bb). Optimal campaign planning/scheduling of multipurpose batch/semi-continuous plants, 2. A mathematical decomposition approach. *Ind. Eng. Chem. Res. 35*, 510.

Petkov, S. B., & Maranas, C. D. (1997). Multiperiod planning and scheduling of multiproduct batch plants under demand uncertainty. *Ind. Eng. Chem. Res. 36*, 4864–4881.

Rodrigues, M. T., Latre, L. G., & Rodrigues, L. C. (2000). Short-term planning and scheduling in multipurpose batch chemical plants: a multi-level approach. *Comput. Chem. Eng. 24* (9/10), 2247.

Sahinidis, N. V., & Grossmann, I. E. (1992). Reformulation of the multiperiod MILP model for capacity expansion of chemical processes. *Operat. Res. 40*, S127–S144.

Sand, G., Engell, S., Märkert, A., Schultz, R., & Schulz, C. (2000). Approximation of an ideal online scheduler for a multiproduct batch plant. *Comput. Chem. Eng. 24*, 361–367.

Shah, N. (1998). Single- and multisite planning and scheduling: current status and future challenges. *AICHE Symp. Ser. No. 320 94*, 75.

Shobrys, D. E., & White, D. C. (2000). Planning, scheduling and control systems: why can they not work together. *Comput. Chem. Eng. 24*, 163–173.

Sood, A. K., Funk, G. L., & Delmastro, A. C. (1971). Dynamic optimization of a natural gas pipeline using a gradient search technique. *Int. J. Contr. 14* (6), 1149–1157.

Sun, C. L., Uraikul, V., Chan, C. W., & Tontiwachwuthikul, P. (1999). An integrated expert system/operations research approach for natural gas pipeline operations optimization. *IEEE Can. Conf. Electr. Comput. Eng. Proc. 2*, 114–1120.

Türkay, M., & Grossmann, I. E. (1996). Logic-based MINLP algorithms for the optimal synthesis of process networks. *Comput. Chem. Eng. 28* (8), 959–978.

Türkay, M., & Grossmann, I. E. (1998). Tight mixed-integer optimization models for the solution of linear and nonlinear systems of disjunctive equations. *Comput. Chem. Eng. 22* (9), 1229–1239.

Van den Heever, S. A., Grossmann, I. E., Edwards, K., & Vasantharajan, S. (2001). A Lagrangean decomposition heuristic for the design and planning of offshore hydrocarbon field infrastructures with complex economic objectives. *Ind. Eng. Chem. Res 40*, 2857.

Viswanathan, J., & Grossmann, I. E. (1990). A combined penalty function and outer-approximation method for MINLP optimization. *Comput. Chem. Eng. 14*, 769.

Wong, P. J., & Larson, R. E. (1968). Optimization of natural-gas pipelines systems via dynamic programming. *IEEE. Trans. Auto. Contr. AC-13* (5), 475–481.